The Canadian Mineralogist
Vol. 42, pp. 563-582 (2004)

DETRITAL PLATINUM-GROUP MINERALS IN RIVERS DRAINING THE EASTERN BUSHVELD COMPLEX, SOUTH AFRICA

THOMAS OBERTHÜR§, FRANK MELCHER, LOTHAR GAST, CHRISTIAN WÖHRL AND JERZY LODZIAK

Federal Institute for Geosciences and Natural Resources (*BGR*), *Stilleweg 2, D-30655 Hannover, Germany*

ABSTRACT

During field work in the eastern Bushveld, more than 6000 grains of platinum-group minerals (PGM) were recovered from alluvial sediments by panning on the farm Maandagshoek and its environs. The grains were investigated by reflected-light microscopy, scanning electron microscopy and electron-microprobe analysis. More than 40 different species of PGM were found. Monophase grains of Pt–Fe alloy are the most common, followed by sperrylite, cooperite, braggite, isomertieite or mertieite I, stibiopalladinite or mertieite II, and Ru–Os–Ir–Pt alloy. Polyphase grains comprise various combinations of one or two of the aforementioned PGM and laurite, sulfides and arsenides of Rh and Pd, and a wide variety of Pd-dominant compounds with As, Sb, Te, Fe, Sn, Pb and Hg, some of which are previously unreported from the Bushveld Complex or even unnamed species. The individual PGM grains show various degrees of attrition. They are mostly unaltered, but the assemblage also contains partly to severely altered grains. The different states of preservation probably point to long-lived, continuous accumulation of the PGM by sedimentological processes. The large grain-sizes of the PGM in the placers (40 μm to 1.6 mm) compared to those of PGM in the Merensky Reef and the UG–2 (generally <50 μm) indicate pronounced sorting by sedimentological processes. The detrital PGM may originate from the Merensky Reef, the UG–2, platiniferous pipes, or still concealed PGE–PGM occurrences. However, grain morphologies, mineralogical association and mineral chemistry of the PGM only allow cautious links with their original sources, which were probably close to the final sites of deposition. The significance of the presence of a large number of both rare and hitherto unreported PGM in the placers is outlined in light of regional mineral exploration and also with respect to the metallurgical treatment of the PGE-bearing ores of the Bushveld Complex. The area of the farm Maandagshoek and environs is a world-unique "hot spot" regarding both the presence of different types of PGE mineralization (Merensky Reef, UG–2, platiniferous pipes, and placers) and the fact that these occurrences are type localities of a considerable number of well-known and also exotic PGM.

Keywords: platinum-group minerals, placer, Maandagshoek, eastern Bushveld Complex, South Africa.

SOMMAIRE

Lors de nos campagnes de terrain dans la partie est du complexe de Bushveld, nous avons prélevé plus de 6000 grains de minéraux du groupe du platine (MGP) des sédiments alluvionnaires par lavage à la batée dans les environs de la ferme Maandagshoek. Nous les avons étudiés par microscopie optique en lumière réfléchie, par microscopie électronique à balayage et par analyse à la microsonde électronique. Plus de 40 espèces de MGP sont présentes. Les grains monophasés d'un alliage Pt–Fe sont les plus communs; suivent ensuite sperrylite, cooperite, braggite, isomertieïte or mertieïte I, stibiopalladinite or mertieïte II, et un alliage à Ru–Os–Ir–Pt. Les grains polyphasés sont faits de diverses combinaisons des MGP déjà cités et de la laurite, des sulfures et arséniures de Rh et Pd, et toute une variété de composés à dominance de Pd, combiné avec As, Sb, Te, Fe, Sn, Pb et Hg, dont certains sont nouveaux à être signalés dans ce complexe ou bien tout simplement nouveaux. Les grains des MGP montrent un degré d'usure variable. La plupart sont sains, mais l'assemblage contient aussi des grains partiellement ou complètement altérés. Les différents états de préservation découlent probablement d'une accumulation continue, à long terme, des MGP par processus sédimentologiques. La taille relativement grande des MGP dans les placers (40 μm jusqu'à 1.6 mm), comparée à la taille des grains dans le banc de Merensky ou dans l'unité UG–2 (généralement <50 μm) serait le résultat d'un triage efficace dû à ces processus sédimentologiques. Les MGP détritiques pourraient provenir du banc de Merensky, de l'unité UG–2, des conduits verticaux (pipes) platinifères, ou bien encore d'indices de MGP enfouis. Toutefois, la morphologie des grains, l'association minéralogique et la composition des minéraux permettent seulement des liens provisoires avec les sources originales, qui étaient tout probablement proximales. Nous explorons la raison d'être d'une telle variété d'espèces rares ou encore méconnues dans les placers en termes d'une campagne d'exploration minérale et aussi par rapport au traitement métallurgique des minerais platinifères de ce complexe. Cette région sur la ferme Maandagshoek et ses environs est un "point chaud" unique au

§ *E-mail address*: thomas.oberthuer@bgr.de

monde par rapport à la présence de différents modes de minéralisation en éléments du groupe du platine, et aussi parce que ces indices sont la localité type de plusieurs espèces de MGP bien connus et d'autres plutôt exotiques.

(Traduit par la Rédaction)

Mots-clés: minéraux du groupe du platine, placer, Maandagshoek, partie est du complexe de Bushveld, Afrique du Sud.

Introduction

The initial major discovery of platinum in the Bushveld Complex, which subsequently led to the discovery of the Merensky Reef, was made in 1924 by panning in a river bed on the farm Maandagshoek in the Eastern Bushveld (Merensky 1924, 1926, Wagner 1929). Wagner (1929) also reported on a number of alluvial diggings in the Bushveld Complex that produced unknown amounts of platinum. However, as mining commenced on the rich pipes and reef-type deposits of the Bushveld, alluvial PGM soon became forgotten, and no published information on the mineralogical nature of the placer PGM is available. Cawthorn (1999, 2001) performed geochemical investigations of stream sediments in the vicinity of the 1924 discovery site and found Pt concentrations ranging up to 0.79 ppm. Guided by Grant Cawthorn, we performed reconnaissance sampling in the Eastern Bushveld (Gast & Wittich 2001, Oberthür *et al.* 2002b, Weiser 2002), followed by SEM and electron-microprobe studies. In the present work, we provide a first comprehensive description of the assemblage of detrital PGM found on the farm Maandagshoek in the eastern Bushveld. A second paper in preparation will concentrate on alteration features of the detrital PGM.

Regional Geology and Geomorphology

Our sampling focused on stream sediments of rivers in the vicinity of the original discovery site of the Merensky Reef, on the farm Maandagshoek, close to Burgersfort in the Eastern Bushveld (Figs. 1, 2). Some of the localities investigated by Cawthorn (1999, 2001), *i.e.*, those documented by Merensky (1924) as being Pt-bearing, and additional sites along the Moopetsi River, were sampled. The river valley is between 2 and 3 km wide and runs approximately north–south, subparallel to the layering of the Mafic Phase of the Bushveld Complex. To the west are the Leolo Mountains, composed of Main Zone gabbros, which overlie the Critical Zone and the Merensky Reef. To the east lies another chain of hills underlain by the Critical Zone. Between the Atok mine and Steelpoort (Fig. 2), the layered sequence dips 10–15° southwest and west. To the east of the Moopetsi River valley is a second parallel valley. According to Cawthorn (2001), the existence of two valleys, less than 5 km apart, may well be the result of glacial activity during the Permo–Carboniferous period. Cawthorn (2001) further assumed that Permian to Jurassic sedimentary rocks (Karoo) had infilled the entire area, but the valleys have been exhumed to close to their original glacial morphology, exposing the bedrock in places. Significant rivers in these two valleys originally flowed southward, depositing considerable alluvium in the valleys. As a result of the recent uplift to the east (Partridge 1998), which has produced the Drakensberg escarpment, and also to the drying of the climate, both rivers now contain a watershed running northeast–southwest across the river valley on the farm Maandagshoek (Fig. 2). Accordingly, both a north- and a south-flowing Moopetsi River are present. In the area of the watershed, thick sediments of sand-supported gravels are present. On the farm Maandagshoek, both the Merensky Reef and the UG–2 strike approximately north–northeast, are about 2 km apart, and crop out on the western and eastern side, respectively, of the Moopetsi River valley. Smaller ultramafic pipes occur to the east, and the better-known Driekop, Mooihoek and Onverwacht pipes are exposed to the north and southeast, respectively (Fig. 2).

These opposing streams on Maandagshoek (both called the Moopetsi River) are now reworking the Recent (or even older ?), poorly consolidated sediments that had accumulated prior to uplift. The outcrops of both the Merensky Reef and the UG–2 horizon can be traced from close to the Atok mine for over 30 km to the Steelpoort River (Fig. 2). Hence, the original, larger, southward-flowing river could have eroded platinum-group elements (PGM) liberated by weathering from the Merensky Reef, the UG–2 and other chromitite seams, and a number of platiniferous pipes.

Samples and Methods

Most PGM grains (~98% by number) were found in the southward-flowing Moopetsi River and its subsidiary creeks within the limits of the farm Maandagshoek. Between 50 and 100 kg of sand- to gravel-sized samples of sediment each were taken, weighed and sieved at 15 different sampling points. Fractions >2 mm were checked by panning; however, as no PGM or gold grains were detected, this fraction was discarded later, and only the <2 mm fraction was treated further. After weighing, the material was panned to obtain heavy-mineral preconcentrates, which were collected in bottles in the field. Final treatment in the laboratories of BGR comprised panning and sieving into various <2 mm size-fractions, and the investigation of the final concentrates under a binocular microscope. Altogether, a mass of

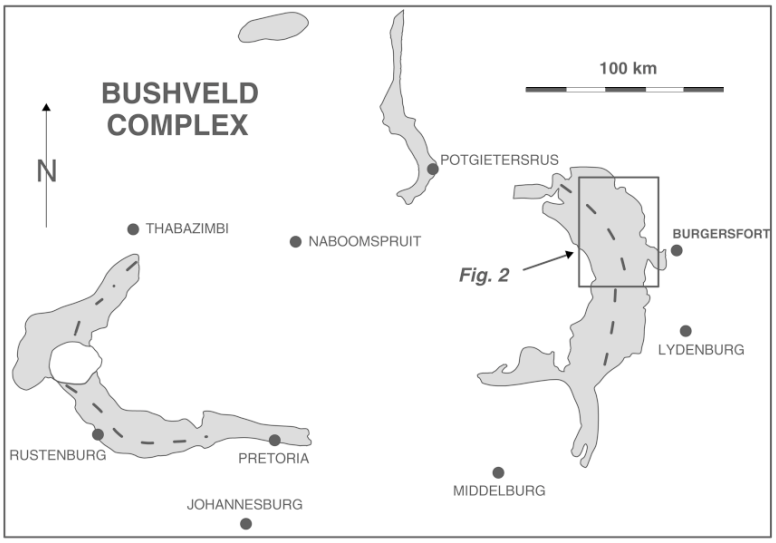

FIG. 1. Geology of the Bushveld Complex showing the exposure of the Mafic Phase (Rustenburg Layered Suite), and outcrop of the Merensky Reef (dashed line). After Cawthorn (2001). Inset shows area depicted in Figure 2.

1127 kg of sediment was treated, resulting in 5.232 kg of pre-concentrates and 6.4 g of final concentrates. The final heavy-mineral concentrates mainly consist of grains of chromite and magnetite (95–99%), followed by grains of ilmenite, rutile, zircon, baddeleyite, monazite, PGM and gold. Altogether, more than 6000 grains of PGM and 406 grains of gold were detected. The richest sample, recalculated to the original sample weight, had a content of 1.29 g PGM/t and 0.13 g Au/t. The largest PGM grain is a Pt–Fe alloy with a true maximum diameter of 1.6 mm (Fig. 3a), and the largest grain of gold is 0.9 mm in diameter.

PGM and gold grains were extracted from the final concentrates by hand, transferred to a sample holder, and studied using a scanning electron microscope (SEM) with an attached energy-dispersion analytical system. In all, 1425 PGM grains were studied this way. Selected PGM grains were mounted, polished sections were prepared, and a total of *ca.* 300 grains of PGM and 16 grains of gold were analyzed using a CAMECA SX100 electron microprobe operated at the following analytical conditions: accelerating voltage 20 kV, specimen current 30 nA, and measurement times 10 or 20 s. The following X-ray lines and standards were used: Os$M\alpha$, Ir$L\alpha$, Pt$L\alpha$, Au$L\alpha$, Ru$L\alpha$, Rh$L\alpha$, Pd$L\alpha/L\beta$, Ag$L\beta$, Fe$K\alpha$, Co$K\alpha$, Ni$K\alpha$, Cu$K\alpha$, Se$L\alpha$, Te$L\alpha$, Bi$M\alpha$, Sn$L\alpha$, and Sb$L\alpha$ (metals), Pd$L\alpha/L\beta$ (synthetic PdS), S$K\alpha$ (synthetic $Pt_{0.7}Pd_{0.3}S$, PdS, and pyrite), and As$L\alpha$ (synthetic GaAs). Raw data were corrected using the PAP program supplied by CAMECA. Additional corrections were performed for enhancement of the elements Rh, Pd, Ag, Cu, As, and Sb by secondary lines. Detection limits of the elements sought are in the order of 0.1 wt.%.

RESULTS: GRAIN MORPHOLOGY

Scanning electron microscope (SEM) investigations are valuable in the study of grain morphologies and allowed us to obtain semiquantitative analytical data for mineral grains. However, SEM analyses are performed on the surfaces of grains only; therefore, thin crusts on the grains or overgrowths may produce compositions that differ from the internal makeup of the grains. Indeed, polished section studies and the electron-microprobe analyses demonstrate that some PGM grains assigned to native Pt or Pt–Fe alloy have a core of cooperite or braggite. This fact must be taken into consideration regarding the PGM proportions obtained by SEM given below.

A semiquantitative overview by SEM (the 1425 PGM grains studied) shows that the PGM assemblage is mainly composed of grains of native Pt, Pt–Fe and Pt–Fe–Cu–Ni alloys (together, 73.2% by number of grains), the Pt and Pd sulfides cooperite and braggite (14.2%) and sperrylite (10.2%). The remainder (2.4%) consists of a variety of rarer PGM. Grain sizes range from 40 μm to 1.6 mm in diameter, and the highest numbers of PGM grains were found in the fraction <125 μm. Besides monomineralic PGM grains, a large number of grains are intergrowths of between two and six different PGM, the most common association being laurite intergrown with grains of Pt–Fe alloy.

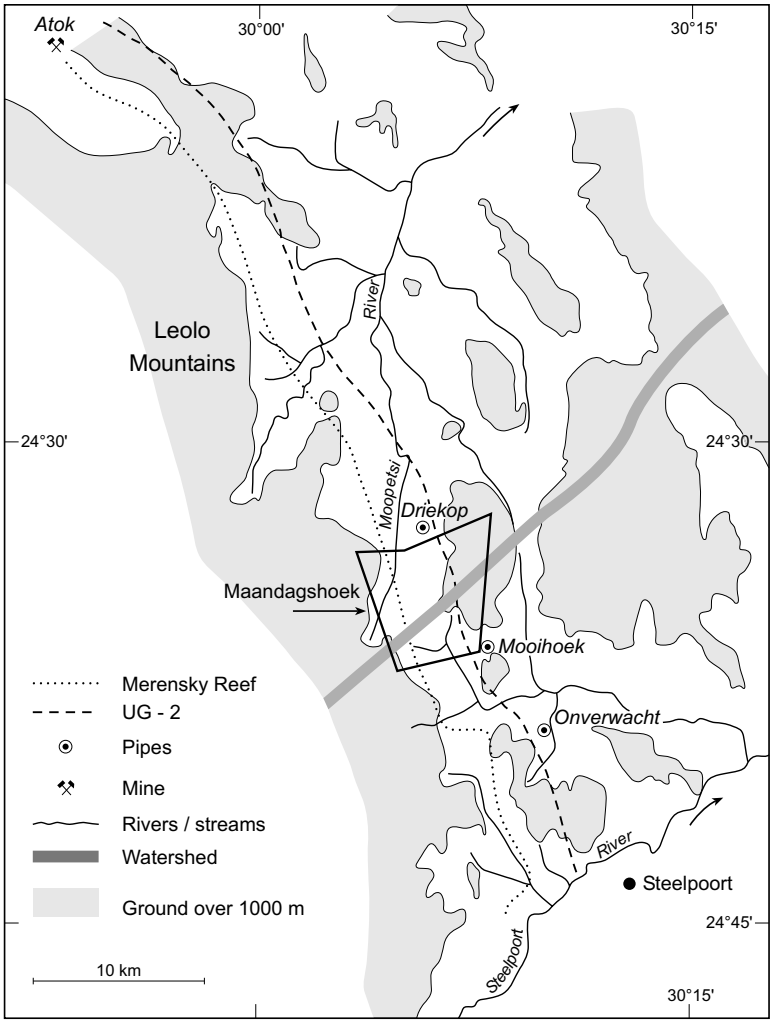

FIG. 2. Geomorphology, geographic location of the farm Maandagshoek, approximate outcrops of the platiniferous horizons (Merensky Reef and UG–2), and location of platiniferous pipes in the Eastern Bushveld. Modified after Gain (1985) and Cawthorn (2001).

Pt–Fe alloy grains are up to 1.6 mm in diameter (mostly between 100 and 200 μm) and have various surface morphologies. Grains with well-rounded shapes (Fig. 3a) are most common, although cubic crystals also are present (Fig. 3b). Intergrowths with laurite embedded in or attached to Pt–Fe alloy grains are common (Fig. 3c), whereas intergrowths with Ru–Os alloy are rare (Fig. 3d). Sperrylite grains are generally multifaceted single crystals without any signs of corrosion or mechanical wear (Fig. 3e). An intergrowth between sperrylite and atheneite was observed in a single grain. The (Pt,Pd) sulfides cooperite and braggite are mainly present as splintered, broken grains (Fig. 3f). Other PGM detected are various alloys of the system Ru–Os–Ir–Pt (invariably intergrown with Pt–Fe alloy), atheneite, stibiopalladinite (Fig. 3g), and some undetermined phases consisting of various combinations of Pt, Pd and Rh with Sb, As, or S. The gold grains are flakes with bent edges or equidimensional grains with smooth surfaces (Fig. 3h).

RESULTS: TEXTURE AND COMPOSITIONS

The frequencies of the PGM investigated by electron microprobe differ slightly from those of the PGM grains investigated by SEM, owing to the preferential

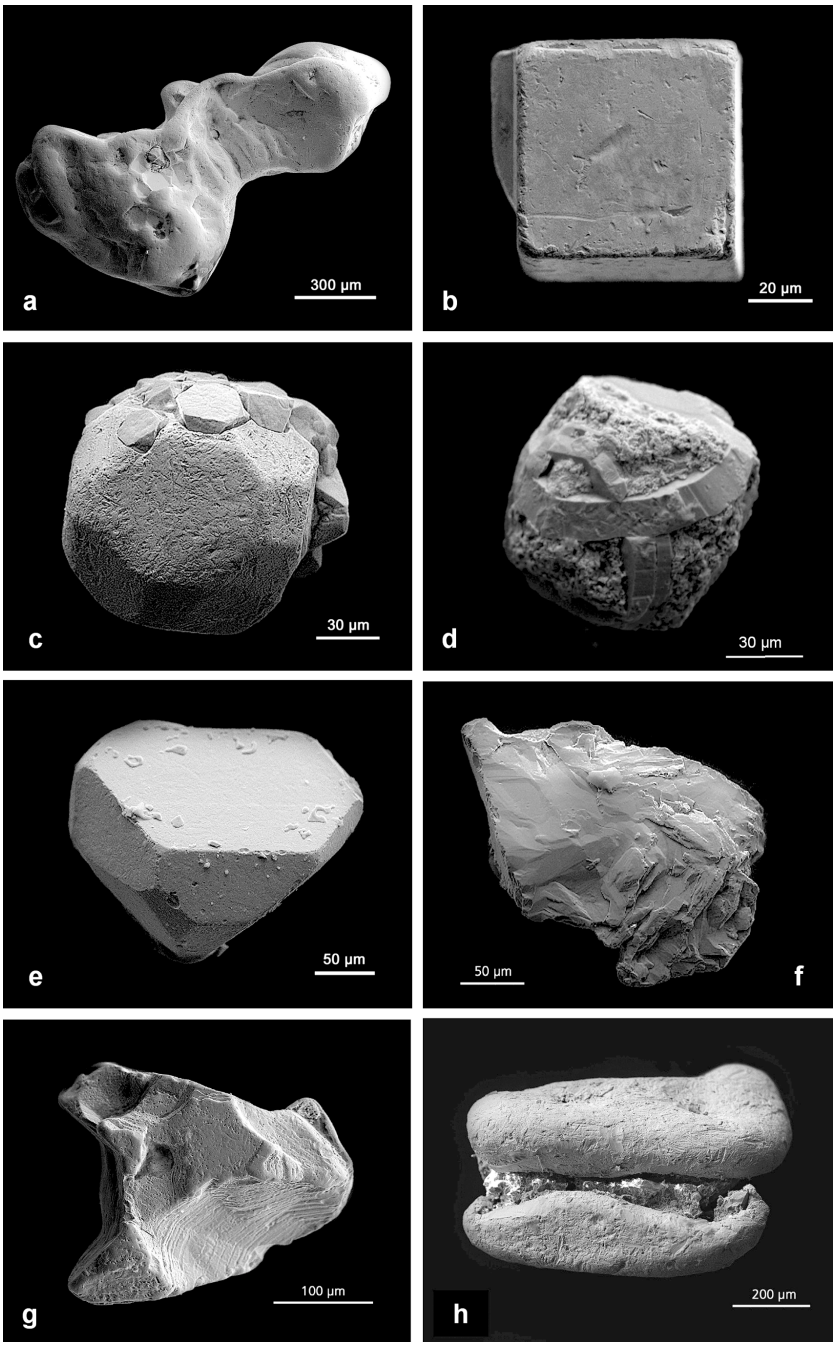

FIG. 3. Scanning electron microscope images (SEM) of individual PGM grains. a) Pt–Fe alloy grain (1.6 mm in diameter) with smooth surface. Grain 9801/SA1005. b) Idiomorphic Pt–Fe alloy grain. Note slightly contorted edges. Grain 9531/SA1004. c) Grain of Pt–Fe alloy showing cubic crystal faces and smooth surface polish, intergrown with platelets of laurite (on top). Grain 9354/SA1004. d) Grain of Pt–Fe alloy transected by plates of Ru–Os alloy. Grain 8339/SA1001. e) Sperrylite crystal showing little attrition. Grain 7747/SA1001. f) Splinter of large grain of cooperite. Grain 9107/SA1002. g) Single grain of isomertiete/mertieite II. Grain 7775/SA1001. h) Large gold grain ("goldburger from Burgersfort") with numerous scratches on the surface and bent and overturned edges enclosing silicates (white). Grain 9935/SA1005.

selection of rarer phases for analysis. The PGM analyzed are variably altered grains of native Pt and Pt–Fe alloy (68% of the grains by number), the Pt–Pd sulfides cooperite and braggite (14%), sperrylite (7%), and other PGM (11%). In contrast to the SEM observations on single PGM grains, which yielded true maximum diameters, the grain sizes given below are apparent maximum diameters measured in polished sections. In the following, the nomenclature and formulae given by Cabri (2002) are adopted for approved PGM, whereas reference is made to Daltry & Wilson (1997) with respect to unnamed or undefined PGM. Table 1 summarizes the PGM detected, their preferred mode of occurrence and estimated frequency by number. The listing roughly follows the sequence PGE alloys, sulfides, sulfarsenides, arsenides, and finally the large variety of palladium minerals. Their general formulae range from [Pd_3X] with 75 at.% Pd to [Pd_8X_3] with 71.4 at.% Pd, and *X* is either Sb, As, Fe, Te, Pb or Sn, or a combination of some of these elements. The list also includes Cu_2PdAu and gold.

TABLE 1. INVENTORY OF DETRITAL PGM IDENTIFIED IN SEDIMENT SAMPLES, FARM MAANDAGSHOEK, EASTERN BUSHVELD COMPLEX

PGM	Ideal formula	single grains	inter-growths	inclusions
Pt-Fe alloy	Pt_3Fe - $Pt_{1.5}Fe$	●●●	●●●	
* Tulameenite	Pt_2CuFe			
* Ferronickelplatinum	Pt_2NiFe			
*	Pt(Fe,Ni,Cu)			
*	$PtNi_2Fe$			
* PGE-oxides, PGE hydroxides				
Native platinum	Pt	●	●	
Ru-Os-Ir-Pt alloy		●	●	○
Pt-Rh alloy			○	
Native rhodium	Rh		○	
Laurite	RuS_2		●●	
Erlichmanite	OsS_2			○
Cooperite	PtS	●	●	
Braggite	(Pt,Pd)S	●●	○	
Bowieite	Rh_2S_3		●	
Miassite	$Rh_{17}S_{15}$		●	
Rh-Fe-Ni-sulfide	$(Rh,Fe,Ni)_3S_8$ (?)		●	
Cuprorhodsite – Malanite	$CuRh_2S_4$ - $CuPt_2S_4$		○	
Vasilite	$Pd_{16}S_7$	○	●	
Hollingworthite	RhAsS		●	
Irarsite	IrAsS		○	
Sperrylite	$PtAs_2$	●●	○	
Rhodarsenide	$(Rh,Pd)_2As$		●	
Palladoarsenide	Pd_2As		●	
Unnamed	RhNiAs		○	
Stillwaterite	Pd_8As_3		○	
Atheneite	$(Pd,Hg)_3As$	○	○	
Stibiopalladinite/Mertieite II	$Pd_{5+x}Sb_{2-x}$ / $Pd_8(Sb,As)_3$	●	●	
Isomertieite/Mertieite I	$Pd_{11}Sb_2As_2$	●	●	
Unnamed	$Pd_{11}Te_2As_2$		●	
Keithconnite	$Pd_{3-x}Te$		○	○
Unnamed	Pd_3Fe		○	○
Zvyagintsevite	Pd_3Pb		○	
Atokite	Pd_3Sn			○
Unnamed	$(Pd,Rh)_3Te_2$			○
Moncheite	$PtTe_2$		○	○
Michenerite	PdBiTe			○
Sobolevskite	PdBi			○
Kotulskite	PdTe			○
Potarite	PdHg	○		○
Unnamed	Pd(Cu,Te)	○		
Unnamed	Cu_2PdAu		○	
Gold	Au	●●	○	○

Relative frequencies are: ●●●: very common, ●●: common, ●: rare, ○: very rare.
*: Alteration phases to be described in a paper in preparation.

Pt–Fe alloy

About 68% of the PGM consist of single or polyphase, variably altered grains of Pt–Fe alloy. More than 78% of these grains have compositions ranging from [Pt_3Fe] to [$Pt_{1.5}Fe$] ("ferroan platinum"). The remaining 22% are a solid solution of tetraferroplatinum [PtFe], ferronickelplatinum [Pt_2FeNi] and tulameenite [Pt_2FeCu]. Many grains of ferroan platinum are mantled by a phase with the general formula [Pt(Fe,Cu,Ni)], interpreted to be an alteration rim caused by weathering. In many cases, such a rim has an additional outermost rim consisting of a Ni-rich phase close to [Ni_2FePt] in composition. These and other alteration features, briefly mentioned here, are dealt with in detail in the paper now in preparation.

Monophase grains of Pt–Fe alloy are mainly single crystals with variably rounded corners. Polyphase grains of Pt–Fe alloy occur as two textural varieties: (i) as homogeneous grains, part of which have either lamellar or euhedral inclusions of other PGM (Fig. 4a), or (ii) as agglomerates of several PGM (*e.g.*, Figs. 4e, 4f, 5e). In approximate order of abundance, the following minerals are present in polyphase grains: laurite, Rh–Ir sulfides (bowieite–kashinite and miassite), cooperite, braggite, alloys dominated by Ru (most commonly Ru_{70}), Pt or Os (rare), various PGM of the systems Pd – Sb ± As ± Te ± Sn, hollingworthite and irarsite, unnamed [RhNiAs], rhodarsenide or palladoarsenide, unnamed [Pd_3Fe], vasilite, atokite–rustenburgite, cuprorhodsite–malanite, RhNiFe sulfide, and gold (for details see below).

The compositional variation of Pt–Fe alloy grains is shown in Figure 6, and representative results of analyses are given in Table 2. The grains of Pt–Fe alloy are characterized by ΣPGE contents ranging from 56.19 to 74.98 at.%. Most grains have low contents (<2 at.%) of PGE other than Pt; a number of Pt–Fe alloy grains have elevated contents, however, especially of Rh or Pd. Maximum PGE contents (in at.%) are 72.02 Pt, 0.82 Os, 1.55 Ir, 31.21 Pd, 13.76 Rh, and 1.16 Ru. Iron contents range from 24.10 to 36.59 at.% Fe, and limited substitution of Fe by Ni and Cu (up to 5.58 and 5.68 at.%, respectively) is also a relatively common feature.

Native platinum

Native Pt mainly occurs in the form of porous grains (*e.g.*, Fig. 7a), part of which resemble products of alteration of other PGM, as shown for example by included remnants of cooperite or braggite. In addition, a thin film of native Pt occurs at the outermost rim of some grains of sperrylite. Notably, Schneiderhöhn & Moritz (1939) showed texturally similar porous grains of native Pt from oxidized parts of the Merensky Reef and proposed that these grains represent relics of former sperrylite or cooperite grains. The chemical variation of native Pt and

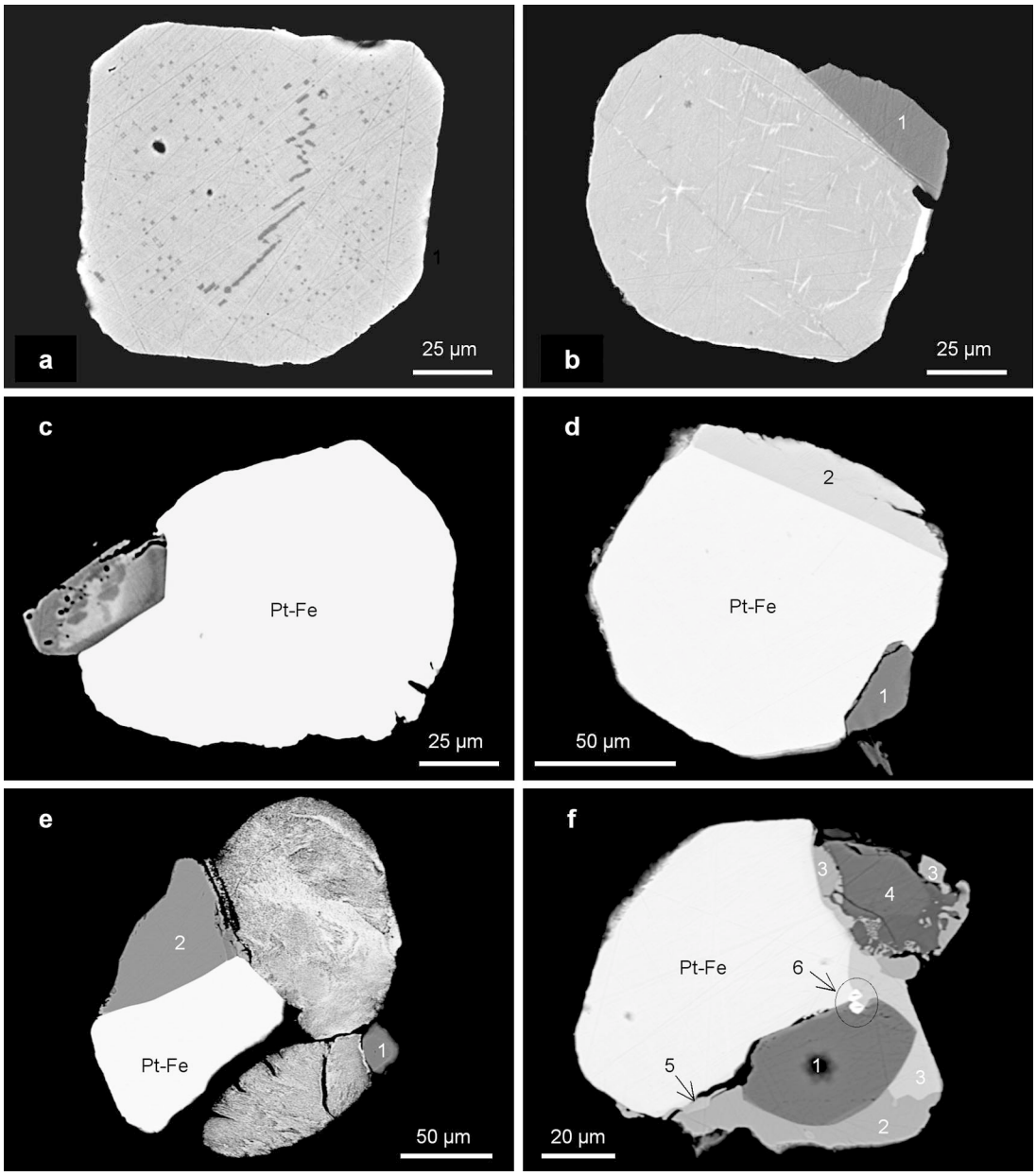

FIG. 4. Back-scattered electron images of PGM in polished sections. a) Grain of Rh-rich Pt–Fe alloy (light grey) with exsolution lamellae of $Pt_{38}Rh_{35}Ru_{20}$ alloy (dark grey). AS6392/107b. b) Grain of Ru-rich Pt–Fe alloy (light grey) with exsolution lamellae of $Ru_{43}Pt_{40}$ alloy (white), and an attached grain of Ru_{70} alloy (1). AS6392/97d. c) Pt–Fe alloy with attached grain of hollingworthite or irarsite. Ir-rich parts are lighter. AS6392/106a. d) Pt–Fe alloy (light grey) with attached grains of laurite (1) and Ru_{73} alloy (2). AS6392/17d. e) Composite grain of compact (left) and porous (bottom and top right) Pt–Fe alloy, intergrown with grains of laurite (1) and bowieite [Rh_2S_3] (2). AS6392/14c. f) Complex grain consisting of Pt–Fe alloy, laurite (1), vasilite [$Pd_{16}S_7$] (2), unnamed [$Pd_{11}Te_2As_2$] (3), RhFeNi sulfide (4) and unnamed [Pd_3Fe] (arrow, 5). Note two small grains of osmium (white, encircled; arrow, 6) on top of the laurite grain. AS 6392/122e.

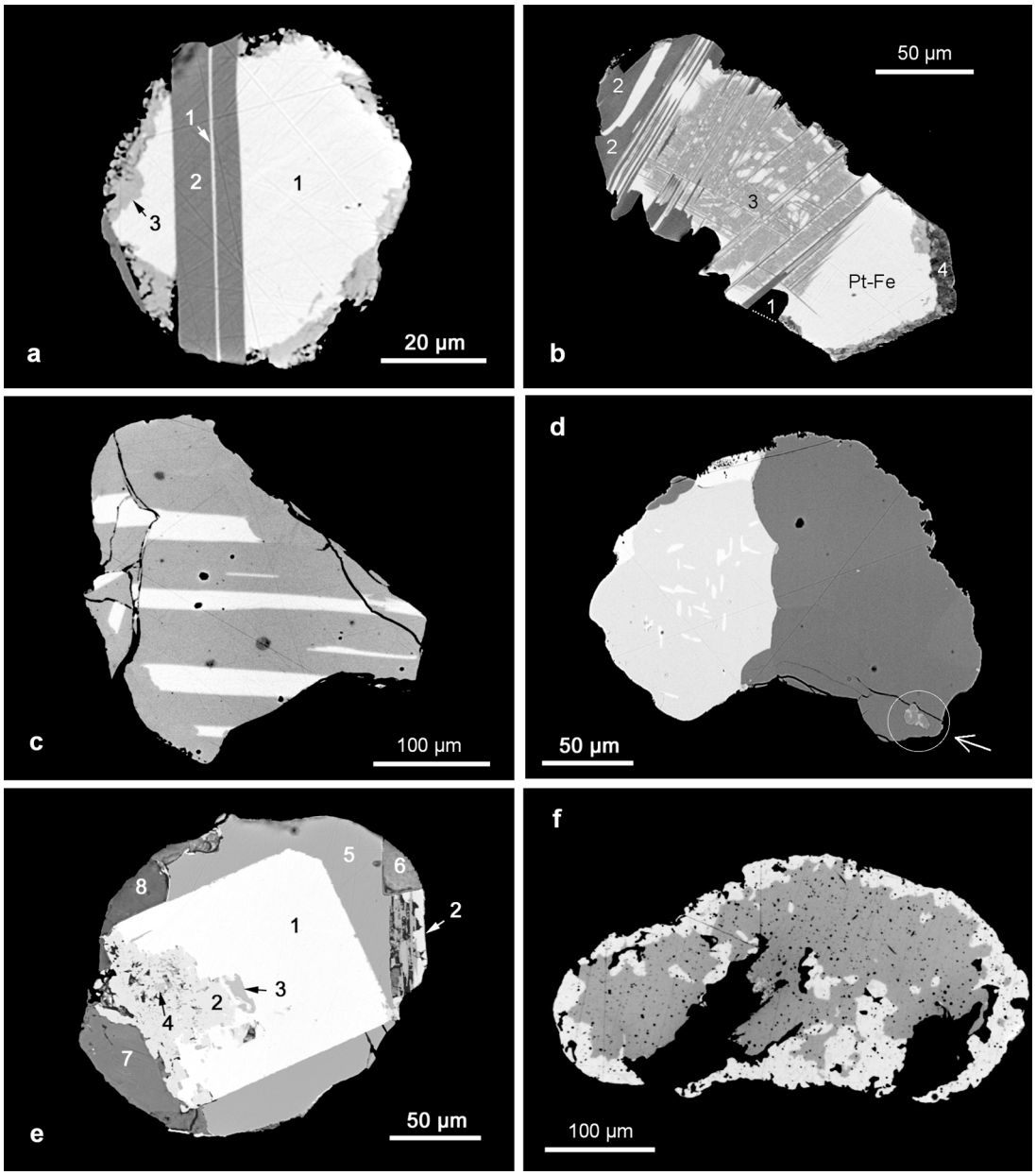

FIG. 5. Back-scattered electron images of PGM in polished sections. a) Polyphase grain of Pt–Fe alloy (1) with a lamellar Ru_{70} alloy (2), overgrown by a rim of [Ni_2PtFe] (3). AS6392/111c. b) Composite grain of Pt–Fe alloy, unnamed RhNiAs (1), Ru_{70} alloy (2), and $Ru_{43}Pt_{28}Rh_{19}$ alloy (3). Note rim of ferronickelplatinum (4) at periphery of Pt–Fe alloy grain. AS6392/67d. c) Grain consisting of isomertieite or mertieite I (groundmass; dark grey) with lamellae of stibiopalladinite/mertieite II (light grey). AS6392/75a. d) Intergrowth of vasilite [$Pd_{16}S_7$] (darkest grey; right part of grain) and unnamed [$Pd_{11}Te_2As_2$] (medium grey), which contains oriented exsolution-induced bodies of keithconnite [$Pd_{3-x}Te$]; white). A roundish inclusion of unnamed [Pd_3Fe] that is locally gold-bearing (3.77 at.% Au) in vasilite is encircled (arrow). AS6444/15a. e) Polyphase grain of Pt–Fe alloy (1), locally corroded by a Cu-rich Pt–Fe alloy and tulameenite (2), and overgrown by unnamed [$Pd_{11}Te_2As_2$](5), an undetermined Pd–Te–Fe–Si oxide or hydroxide (6), iron hydroxide (7) and a Ca–Mn–Fe silicate (8). Inclusions are kotulskite [PdTe](3) and keithconnite [$Pd_{3-x}Te$](4). AS6393/29f. f) Gold grain (medium grey) with silver-poor rim (light grey). AS6392/86a.

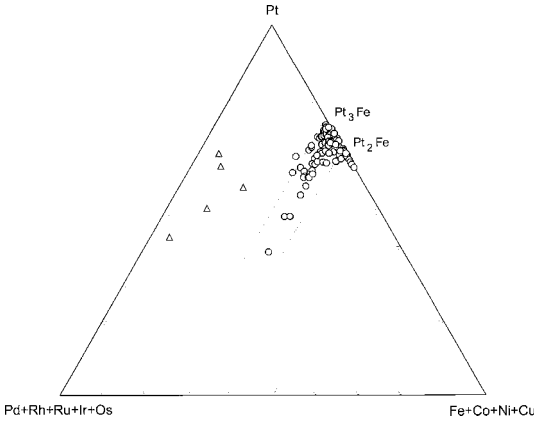

FIG. 6. Compositions (in at.%) of grains of Pt–Pd alloy (triangles), and Pt–Fe alloy (circles), projected in the triangular diagram Pt – (Pd + Rh + Ru + Ir + Os) – (Fe + Co + Ni + Cu).

Pt–Pd alloys is shown in Figure 6, and results of analyses are given in Table 2.

Ru–Os–Ir–Pt–Rh alloy

Altogether, 26 analyses were obtained of multicomponent PGE alloy with compositions in the system Ru–Os–Ir–Pt–Rh. These PGM occur as monomineralic grains, as lamellae in Pt–Fe alloy grains and, more commonly, in polyphase grains mainly intergrown with Pt–Fe alloy (Figs. 4a, 4b, 5a, 5b). Chemically, five groups of Ru–Os–Ir–Pt–Rh alloy are distinguished: (i) Ru-dominant grains (~$Ru_{86–87}Rh_4Pt_1Ni_6Fe_2$, $n = 2$ analyses), (ii) Ru-rich grains (~$Ru_{69–75}Pt_{7–12}Rh_{2–10}Os_{3–9}Ir_{5–7}$, $n = 14$), (iii) Ru-rich grains ($Ru_{69}Os_{19}Ir_9Rh_6Pt_5$, $n = 1$), (iv) Ru–Pt–Rh grains (~$Ru_{43}Pt_{28–40}Rh_{10–20}Ir_3Os_2Fe_{2–3}$, $n = 3$), and (v) Os-rich grains (~$Os_{58–83}Ir_{6–13}Ru_{2–18}Rh_{1–7}Pt_{0–4}$, $n = 6$). The multicomponent PGE alloy compositions are unusual in general; in particular, Ru-rich alloys were so far reported only by Merkle (1998) from

TABLE 2. COMPOSITION OF Pt-Fe ALLOY, NATIVE Pt, AND Ru-Os-Ir-Pt-Rh ALLOY FOUND IN RIVERS DRAINING THE EASTERN BUSHVELD COMPLEX

Sample	Anal.	Fe	Co	Ni	Cu	Ru	Rh	Pd	Sb	Os	Ir	Pt	Hg	Σ
AS6392	177	9.33				0.81	9.72				0.24	80.25		100.34
AS6392	11	10.15		0.31	0.93			0.36				88.80		100.55
AS6392	12			1.77				19.45		0.11		79.36	0.19	100.88
AS6392	62	2.27			0.16	9.12	9.04			1.69	1.95	76.19		100.44
AS6435	21	0.77		0.40				5.49				92.81		99.47
AS6392	176	2.04				15.02	26.52			0.79	1.91	55.22		101.50
AS6392	106	1.30				33.21	15.61			3.15	4.81	43.24	0.14	101.46
AS6392	29/30	0.18				62.24	3.44			11.64	11.36	12.56		101.42
AS6392	144	0.13				59.36	4.85			9.38	8.88	19.30		101.89
AS6444	100	0.88	0.41	3.77		91.17	3.95					2.25		102.43
AS6465	15	0.25				61.96	2.21		0.58	11.48	10.93	12.29		99.70
AS6392	170	0.13				1.98	3.92			79.68	14.35	1.07		101.12
AS6392	211	0.12				11.06	2.06			77.38	7.22	2.91		100.76
AS6465	33	0.28				1.94	89.94		0.45		0.44	3.58	0.20	96.83
AS6435	5	2.39			0.15	9.59	18.08			1.43	2.80	66.51		100.95
AS6392	177	24.49				1.17	13.85				0.18	60.31		100.00
AS6392	11	27.52		0.81	2.22			0.51				68.94		100.00
AS6392	12	0.00		4.85				29.43		0.09		65.48	0.15	100.00
AS6392	62	6.46			0.41	14.30	13.93			1.41	1.61	61.89		100.00
AS6465	43	2.50		1.23				9.42				86.85		100.00
AS6392	176	4.93				20.08	34.84			0.56	1.34	38.25		100.00
AS6392	106	3.03				42.81	19.77			2.16	3.26	28.88	0.09	100.00
AS6392	29/30	0.38				73.55	3.99			7.31	7.06	7.69		100.00
AS6392	144	0.27				70.65	5.68			5.93	5.56	11.91		100.00
AS6444	99/100	1.52	0.65	6.18		86.85	3.69					1.11		100.00
AS6465	15	0.54				74.40	2.60		0.58	7.33	6.91	7.65		100.00
AS6392	170	0.41				3.50	6.81			74.93	13.35	0.99		100.00
AS6392	211	0.38				18.52	3.39			68.84	6.36	2.53		100.00
AS6465	33	0.55				2.08	94.64		0.40		0.25	1.98	0.11	100.00
AS6435	5	6.30			0.34	13.98	25.89			1.11	2.15	50.23		100.00

S, As, Se, Ag, Sn, Te, Au, Pb, Bi and free fields: below detection limits. Compositions, derived from electron-microprobe analyses, are first expressed in weight %, then in atom %.

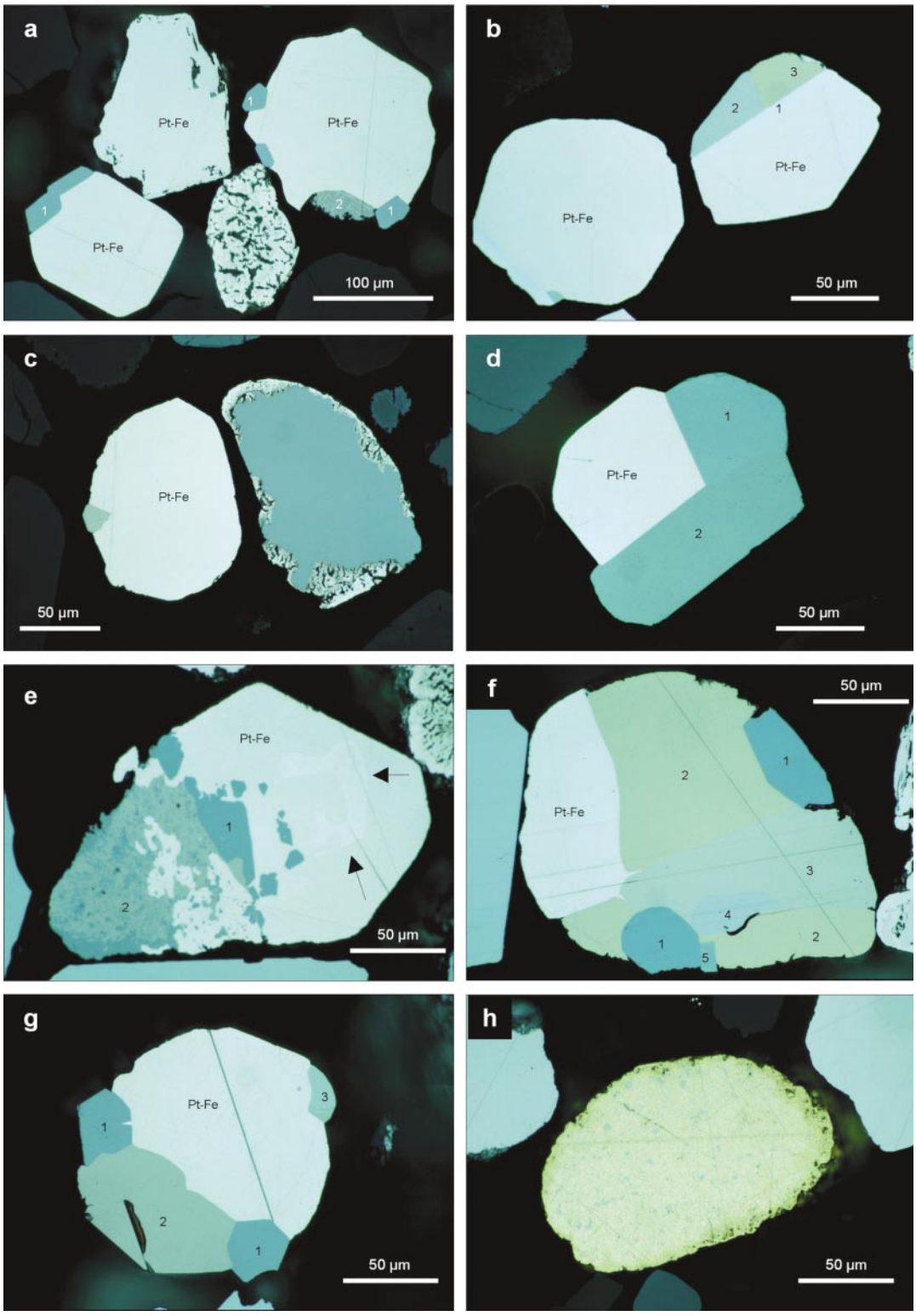
a
Pt-Fe
Pt-Fe
Pt-Fe
1
2
100 µm
b
Pt-Fe
Pt-Fe
50 µm
c
Pt-Fe
50 µm
d
Pt-Fe
50 µm
e
Pt-Fe
50 µm
f
Pt-Fe
50 µm
g
Pt-Fe
50 µm
h
50 µm

the UG–1 chromitite of the Bushveld Complex and by Zaccarini *et al.* (2002) from the Onverwacht and Tweefontein pipes, where the compositional range is ($Ru_{77–80}Os_{5–8}Ir_{4–8}Pt_{6–7}Rh_{2–3}$). The compositional variation of the various Ru–Os–Ir–Pt–Rh alloys is shown in Figures 8a and 8b, and representative compositions are given in Table 2.

Pt–Rh alloy

An amoeboid, inhomogeneous body, about 50 μm in diameter, with the composition $Pt_{50}Rh_{27}Ru_{18}Fe_9$, was observed in a 200 μm grain of $Pt_{64}Rh_{10}Fe_{22}$ alloy, which is furthermore intergrown with laurite and miassite (Fig. 7e).

Rhodium

A slightly inhomogeneous, locally porous grain, 30 μm in diameter, with the composition $Rh_{95}Pt_2Ru_2$, was detected, attached to a larger grain of Pt–Fe alloy. According to the textural appearance of this grain, it may represent an alteration product of a rhodium sulfide.

Laurite

Laurite mostly occurs as idiomorphic grains attached to grains of Pt–Fe alloy, and is occasionally also found in complex intergrowths with Rh sulfides and Ru-rich alloys (Figs. 3c, 7a, 4d, 4e, 4f). Chemically, the mineral is mainly close to ideal RuS_2 in composition, although a number of grains are zoned, having either an Os-rich rim (erlichmanite component), or they show patchwork patterns of Os-rich and Os-poor zones. Maximum contents of other elements are 7.52 at.% Os, 4.70% Ir, 0.52% Pt, 6.37% Rh, and exceptionally, 7.30% As (arsenic contents are quite commonly encountered, but usually below 1 at.%).

Erlichmanite

Two roundish inclusions of erlichmanite [OsS_2], about 10 μm across, were detected in a grain of Pt–Fe alloy. Chemically, these grains of erlichmanite have distinct contents of Rh (8.36 at.%), Ir (2.65%), Ru (2.48%), and As (7.03%).

Cooperite and braggite

The Pt–Pd sulfides cooperite and braggite mainly occur as homogeneous grains. Many of the grains are slightly to severely corroded and rimmed by a variably thick, usually porous layer of native Pt that is crystallographically oriented following orientations of the cooperite or braggite lattice. The grains of native Pt may contain several wt.% Pd, which might indicate removal of Pd and S during weathering (*e.g.,* Fig. 7c). Rare intergrowths with the Rh sulfides miassite or bowieite, and laurite were observed in polyphase grains.

Cooperite compositions are quite uniform (maximum 1.46 at.% Ni and 4.38% Pd). All braggite grains show substantial incorporation of nickel (2.64–10.18 at.% Ni) and are Pd-rich (maximum 20.51 at.% or 25.39 wt.% Pd). This might indicate that the braggite grains originated from the Merensky Reef, because Verryn & Merkle (1994, 2002) reported a limited range of compositions of primary Pt–Pd sulfides from the Merensky Reef (between 14 to 32 wt.% Pd), compared to a wide compositional range down to vysotskite [PdS] from the UG–2 horizon.

Miassite [$Rh_{17}S_{15}$] and *bowieite* [Rh_2S_3]

Two chemically different Rh sulfides are present, corresponding to miassite [$Rh_{17}S_{15}$] and members of the bowieite [Rh_2S_3] – kashinite [Ir_2S_3] solid-solution series. Miassite is found as discrete, homogeneous grains up to 110 μm in diameter, attached to grains of Pt–Fe alloy. Bowieite grains may reach up to 100 μm in diameter in polyphase grains intergrown with Pt–Fe alloy and laurite (Fig. 4e), or are present in simple intergrowths with Pt–Fe alloy, or together with Pt–Fe alloy, cooperite, laurite, and hollingworthite. In addition, both Pt-bearing miassite and Ir-bearing bowieite grains, 20 and 35 μm in diameter, were found in a polyphase grain intergrown with cooperite and laurite.

Chemically, miassite carries elevated contents of Pt, up to 6.10 at.% and 0.91% Ir. The bowieite grains show substantial substitution of Rh by Ir (kashinite component, reaching up to 13.98 at.% Ir). Pt contents are low

FIG. 7. PGM grains in polished sections of heavy-mineral concentrates. Dark grey minerals are mainly chromite and magnetite. Sample SA 1016, Maandagshoek. All photomicrographs taken in oil immersion. a) Three grains of Pt–Fe alloy (Pt–Fe), with attached laurite (1) and RhFeNi sulfide (2). Porous grain (lower half, center) is native platinum. b) Two grains of Pt–Fe alloy, the one to the right has 10 at.% Pd and is intergrown with $Ru_{74}Os_7Ir_7Pt_7$ alloy (1), palladoarsenide [$(Pd,Rh)_2As$] (2) and unnamed [$Pd_{11}Te_2As_2$] (3). c) Grain to the left is Pt–Fe alloy with attached miassite [$Rh_{17}S_{15}$], and grain to the right is cooperite [PtS], which shows a peripheral rim of native platinum (white). d) Composite grain consisting of Pt–Fe alloy, laurite (1) and cuprorhodsite–malanite (2). e) Grain of Pt–Fe alloy (10 at.% Rh) with amoeboid body of $Pt_{50}Rh_{27}Ru_{18}Fe_9$ alloy (arrows), intergrown with coarser laurite (1) and symplectitic mixture (2) of miassite [$Rh_{17}S_{15}$] and laurite. f) Composite grain consisting of Pt–Fe alloy, laurite (1), unnamed [$Pd_{11}Te_2As_2$] (2), palladoarsenide [$(Pd,Rh)_2As$] (3), sperrylite (4), and irarsite (5). g) Composite grain of Pt–Fe alloy intergrown with laurite (1), miassite (2) and rhodarsenide [$(Rh,Pd)_2As$] (3). h) Gold grain with silver-poor rim (darker) and numerous small inclusions of atokite [Pd_3Sn].

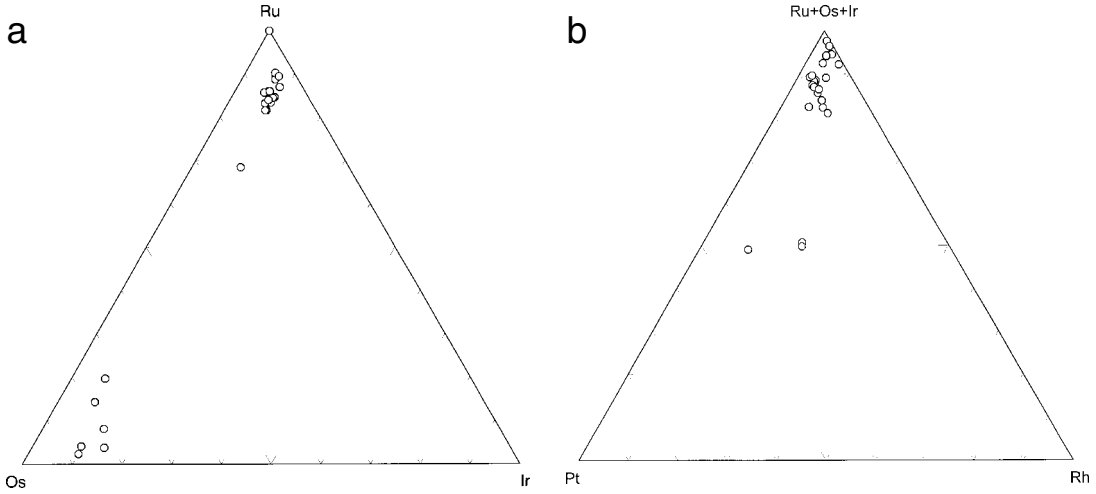

FIG. 8. a) Compositions (in at.%) of Ru–Os–Ir–Pt–Rh alloys, projected in the triangular diagram Ru – Os – Ir. b) Compositions (in at.%) of Ru–Os–Ir–Pt–Rh alloys, projected in the triangular plot (Ru + Os + Ir) – Pt – Rh.

(up to 0.56 at.% Pt). Representative results of analyses of the Rh sulfides are given in Table 3.

Rh–Fe–Ni sulfide

The undetermined Rh–Fe–Ni sulfide was observed in a number of polyphase grains, *e.g.*, in a complex intergrowth together with Pt–Fe alloy, laurite, unnamed [$Pd_{11}Te_2As_2$], vasilite, and unnamed [Pd_3Fe] (Fig. 4f), or at the periphery of Pt–Fe alloy grains and grain aggregates in a partial rim 10–30 μm wide. The mineral reaches sizes up to 40 × 100 μm. Chemically, the Rh–Fe–Ni sulfide most probably corresponds to a monosulfide [(Rh,Fe,Ni)S] or [$RhFeNiS_3$], or to rhodian pentlandite [$(Rh,Fe,Ni)_9S_8$], which was reported as a constituent of complex Pt–Fe nuggets from Yubdo, Ethiopia (Cabri *et al.* 1981). The large number of undetermined Pt – Rh ± Ir ± Fe ± Ni sulfides reported in the literature on the primary Bushveld ores (Merensky Reef and UG–2; Vermaak & Hendricks 1976, Cousins & Kinloch 1976, Kingston & El-Dosuky 1982, Kinloch 1982, McLaren & De Villiers 1982, Mostert *et al.* 1982, Hey 1999, Cawthorn *et al.* 2002) probably are all various PGE – base-metal monosulfides. Notably, a Rh–Fe monosulfide does not exist in the ternary system Rh–Fe–S at temperatures above 500°C (Makovicky 2002). Compositions are presented in Table 3.

Cuprorhodsite [$CuRh_2S_4$] – *malanite* [$CuPt_2S_4$]

Rare grains with compositions pointing to members of the cuprorhodsite [$CuRh_2S_4$] – malanite [$CuPt_2S_4$] solid-solution series (Melcher 2000) reach up to 160 μm in length and occur in composite grains together with Pt–Fe alloy and laurite (Fig. 7d), and with other PGM. The various Pt–Rh–Ir–Cu sulfides reported in the literature on the primary Bushveld ores (Merensky Reef and UG–2; same references as above) are probably all members of the cuprorhodsite – cuproiridsite – malanite solid-solution series. Compositions are given in Table 3.

Vasilite [$Pd_{16}S_7$]

A PGM with composition close to [$(Pd,Cu)_5S_2$] probably is vasilite (Atanasov 1990, Cabri 2002). The mineral is present in many polyphase grains. For example, it reaches a size of 60 μm in an intergrowth with Pt–Fe alloy, laurite, unnamed [$Pd_{11}Te_2As_2$], unnamed RhFeNi sulfide, and unnamed [Pd_3Fe] (Fig. 4f). A grain of vasilite 200 μm across contains a roundish inclusion of unnamed [Pd_3Fe] that is locally gold-bearing (3.77 at.% Au), and is intergrown with unnamed [$Pd_{11}Te_2As_2$] that contains lamellae of keithconnite [$Pd_{3-x}Te$] (Fig. 5d). According to Cabri (2002), vasilite is the natural cuprian analogue of synthetic [$Pd_{16}S_7$], which has an extensive solid-solution field into the system Pd–Cu–S at 550°C (Karup-Møller & Makovicky 1999). Representative compositions are given in Table 3.

Hollingworthite [RhAsS] – *irarsite* [IrAsS]

Hollingworthite and, less commonly, irarsite (Fig. 7f), usually occur as a component of polyphase grains or, in rare cases, are attached to grains of Pt–Fe alloy (Fig. 4c). Hollingworthite grains commonly tend to show idiomorphic crystal faces and may be slightly zoned, having an Ir-rich core and a Rh-rich rim. Grain sizes usually range between 20 and 40 μm.

TABLE 3. COMPOSITIONS OF PGE SULFIDES FOUND IN RIVERS DRAINING THE EASTERN BUSHVELD COMPLEX

Sample	Analysis	Mineral	S	Fe	Co	Ni	Cu	As	Rh	Pd	Ag	Ir	Pt	Bi	Σ
AS6392	153/154	Miassite	19.06					0.12	63.39	0.12		1.26	15.15		99.09
AS6465	48	Miassite	21.03	0.38		0.11	0.47		73.02			1.12	3.05		99.18
AS6392	168	Bowieite	24.75						37.33			35.72	1.45		99.25
AS6392	191	Bowieite	28.01						63.98	0.11		5.30	0.90		98.31
AS6392	206/207	Rh-Fe-Ni sulfide	28.00	16.86	0.20	14.91	4.90		27.45	0.24	0.15	6.80	0.08		99.59
AS6465	8/9	Rh-Fe-Ni sulfide	30.05	20.21	0.65	9.02	3.59		27.69	0.73		5.60	0.95		98.48
AS6467	29	Rh-Fe-Ni sulfide	30.49	18.73	0.13	12.34	4.58		29.55	0.23		2.53	0.31		98.90
AS6465	2	Cuprorhodsite	27.60	1.36			11.93		26.06			1.78	29.57		98.30
AS6467	45	Cuprorhodsite	31.16	6.63			7.83		51.18		0.25		1.62		98.67
AS6467	28	Vasilite	11.89	1.00			6.34			78.41			0.32	0.11	98.07
AS6444	28/154	Vasilite	11.09	1.29			6.32			80.54	0.10			0.12	99.47
AS6392	153/154	Miassite	14.66					0.04	15.20	0.03		0.16	1.92		32
AS6465	48	Miassite	14.96	0.16		0.04	0.17		16.19			0.13	0.36		32
AS6392	168	Bowieite	2.91						1.37			0.70	0.03		5
AS6392	191	Bowieite	2.86						2.03			0.09	0.02		5
AS6392	206/207	Rh-Fe-Ni sulfide	1.01	0.32		0.27	0.08		0.28			0.04			2
AS6465	8/9	Rh-Fe-Ni sulfide	1.02	0.40	0.01	0.17	0.06		0.29	0.01		0.03	0.01		2
AS6467	29	Rh-Fe-Ni sulfide	1.01	0.36		0.22	0.08		0.31			0.01			2
AS6465	2	Cuprorhodsite	4.05	0.11			0.88		1.19			0.04	0.71		7
AS6467	45	Cuprorhodsite	3.95	0.48			0.50	0.00	2.02		0.01		0.03		7
AS6467	28	Vasilite	6.95	0.33			1.87			13.81			0.03	0.01	23
AS6444	28/154	Vasilite	6.48	0.43			1.87			14.19	0.02			0.01	23

Se, Ru, Sn, Sb, Te, Os, Au, Hg, Pb, Bi and free fields: below detection limits. Compositions, derived from electron-microprobe analyses, are first expressed in weight %, then in atoms per formula unit, with the sum of atoms shown in the last column.

Sperrylite

Sperrylite mainly occurs in the form of unaltered monophase crystals. Intergrowths in complex grains with other PGM are rare (Fig. 7f). The mineral is close to being stoichiometric [$PtAs_2$] in composition. Maximum contents of other elements recorded in sperrylite are 2.53 at.% S, 0.31 at.% Se, and 1.99 at.% Sb, respectively.

Rhodarsenide [$(Rh,Pd)_2As$] – *palladoarsenide* [Pd_2As]

A number of grains of Rh–Pd arsenide were detected. One grain, 12 μm in diameter, was found included in laurite intergrown with a grain of $Pt_{76}Ru_9Rh_9Fe_2$ alloy; other grains (30 and 35 μm in diameter) are attached to Pt–Fe alloy. In addition, smaller grains (up to about 10 μm in diameter) were found as a thin film at the boundary between a grain of tulameenite and a capping of porous iron hydroxides, which also contains irregular, small grains of zvyagintsevite [Pd_3Pb]. A blade-like grain of palladoarsenide 150 μm long occurs in the multiple intergrowth shown in Figure 7f, together with Pt–Fe alloy, unnamed $Pd_{11}Te_2As_2$, laurite, sperrylite and irarsite.

Electron-microprobe analyses indicate a range of compositions from the end member [Rh_2As] to [$(Pd>Rh)_2As$]. In contrast to Cabri (2002), who used the formula [$(Rh,Pd)_2As$] for rhodarsenide, the ideal formula of rhodarsenide should be written [Rh_2As]. Altogether, the grains analyzed fit into the range of *rhodarsenide* (orthorhombic [$(Rh,Pd)_2As$]; Tarkian *et al.* 1997) – *palladoarsenide* (monoclinic [Pd_2As]; Begizov *et al.* 1974) – *palladodymite* (orthorhombic [$(Pd,Rh)_2As$]), which may form a complete solid-solution series (Cabri 2002). Representative compositions are given in Table 4.

Unnamed [RhNiAs]

This PGM was found (i) as a 20 μm grain at the rim of a grain of Pt–Fe alloy, (ii) as a 15 μm grain at the rim of a complex grain of Pt–Fe alloy intergrown with $Ru_{43}Pt_{28}Rh_{19}Fe_3$ alloy and $Ru_{71}Rh_9Pt_9$ alloy (Fig. 5b), and (iii) as a homogeneous, 40 μm large grain attached to a grain of Pt–Fe alloy. Chemically, the mineral is close to [RhNiAs] in composition (Table 4). A chemically similar PGM was reported by Hagen *et al.* (1990) from placers in Burma. The unnamed [RhNiAs] may be the Rh-dominant analogue of majakite [PdNiAs].

Stillwaterite [Pd_8As_3]

A large grain (90 μm long) of stillwaterite was found in a complex aggregate consisting of a Pd-rich (10 at.% Pd) Pt–Fe alloy, unnamed [$Pd_{11}Te_2As_2$], cuprorhodsite and laurite, and as a 70 μm large grain overgrowing a grain of Pt–Fe alloy intergrown with unnamed [$Pd_{11}Te_2As_2$] and hollingworthite. A representative composition is given in Table 4.

Atheneite

Individual detrital grains of atheneite [$(Pd,Hg)_3As$] are rare and were only observed in the concentrates by SEM studies. Intergrowths comprise atheneite with sperrylite, and atheneite with Pt–Fe alloy, hollingworthite and zvyagintsevite.

Stibiopalladinite [$Pd_{5+x}Sb_{2-x}$] and *mertieite II* [$Pd_8(Sb,As)_3$]

According to Cabri (2002), stibiopalladinite (hexagonal) and mertieite II (rhombohedral) are "related". The two PGM are dealt with together owing to the fact that a distinction between these PGM by both optical and chemical means is difficult. Both minerals are cream-yellow to yellowish white and variably anisotropic. Cabri (2002) noted that Sb contents per formula unit range from about $Sb_{1.26}$ to $Sb_{1.95}$ in stibiopalladinite, and that the ratio Sb:(As,Te,Sn,Bi,Pb) is usually 5:1 in mertieite II.

Stibiopalladinite or mertieite II occurs (i) as large, homogeneous, monomineralic single grains, up to 350 μm in diameter, (ii) in simple or oriented intergrowths with (Fig. 5c) or attached to isomertieite or mertieite I,

TABLE 4. COMPOSITIONS OF PGE ARSENIDES AND ANTIMONIDES FOUND IN RIVERS DRAINING THE EASTERN BUSHVELD COMPLEX

Sample	Anal.	Mineral	S	Fe	Ni	Cu	As	Se	Rh	Pd	Ag	Sn	Sb	Te	Ir	Pt	Hg	Bi	Σ
AS6392	64	Rhodarsenide	0.14				24.57		72.02	0.80						1.97			99.50
AS6392	139	Palladoarsenide					22.63		35.49	38.64			0.35	1.99		0.24			99.34
AS6465	24	Stillwaterite				0.17	17.05	0.11		77.43		0.22	1.48	1.44			0.15	0.17	98.23
AS6392	102	[RhNiAs]*		0.11	23.49	2.80	26.09		41.29	4.59			2.25			1.29			101.91
AS6444	92	Stibiopalladinite/ mertieite II		0.12		0.15	2.99			69.81		5.84	15.54	3.30		3.35		0.47	101.57
AS6444	161	Stibiopalladinite/ mertieite II					2.73			72.10			25.71		0.26				100.79
AS6444	25	Isomertieite/ mertieite I					8.58			74.57	0.21		15.68						99.04
AS6444	155	Isomertieite/ mertieite I					8.71			74.60	0.16		15.69	0.12					99.27
AS6444	29	[$Pd_{11}Te_2As_2$]*	0.16	0.09			7.34	0.22		74.29		0.36	1.11	16.24				0.46	100.26
AS6467	2	[$Pd_{11}Te_2As_2$]*				0.26	9.58			72.84		0.33	5.33	9.50		0.15		0.78	98.76
AS6467	31	[$Pd_{11}Te_2As_2$]*	0.23				7.15	0.26		72.84		0.95	0.88	15.70		0.22		0.37	98.61
AS6467	14	[$(Pd,Rh)_3Te_2$]*							17.67	37.21				45.42		0.89			101.18
AS6444	30	Keithconnite		0.15			0.25			70.53				28.33		0.23		0.84	100.33
AS6392	64	Rhodarsenide	0.01				0.94		2.00	0.02						0.03			3
AS6392	139	Palladoarsenide					0.88		1.00	1.06			0.01	0.05					3
AS6465	24	Stillwaterite				0.03	2.57	0.02		8.07		0.02	0.14	0.13			0.01	0.01	11
AS6392	102	[RhNiAs]*			0.95	0.10	0.83		0.95	0.10			0.04			0.02			3
AS6444	92	Stibiopalladinite/ mertieite II		0.02		0.02	0.30			4.98		0.37	0.97	0.20		0.13		0.02	7
AS6444	161	Stibiopalladinite/ mertieite II					0.28			5.12			1.60		0.01				7
AS6444	25	Isomertieite/ mertieite I					0.85			5.19	0.01		0.95						7
AS6444	155	Isomertieite/ mertieite I					0.86			5.17	0.01		0.95	0.01					7
AS6444	29	[$Pd_{11}Te_2As_2$]*	0.08	0.03			1.55	0.04		11.06		0.05	0.14	2.01				0.03	15
AS6467	2	[$Pd_{11}Te_2As_2$]*				0.06	2.04			10.90		0.04	0.70	1.19		0.01		0.06	15
AS6467	31	[$Pd_{11}Te_2As_2$]*	0.12				1.54	0.05		11.02		0.13	0.12	1.98		0.02		0.03	15
AS6467	14	[$(Pd,Rh)_3Te_2$]*							0.97	1.98				2.02		0.03			5
AS6444	30	Keithconnite		0.01			0.01			2.96				0.99		0.01		0.02	4

Co, Ru, Os, Au, Pb and free fields: below detection limits. Compositions, derived from electron-microprobe analyses, are first expressed in weight %, then in atoms per formula unit, with the sum of atoms shown in the last column. * Unnamed species.

(iii) as oriented, thin lamellae, up to 30 μm long, in Pt–Fe alloy, (iv) as small (< 20 μm) components in multiphase grains, and (v) as small (<5–20 μm), droplike inclusions, occasionally together with similar inclusions of atokite [Pd_3Sn], in Pt–Fe alloy and tulameenite, and in gold grains. Small (< 5 μm) inclusions of kotulskite [PdTe] were observed in one case in stibiopalladinite or mertieite II.

Chemically, ΣPGE ranges from 71.69 to 73.79 at.%, and Pd contents range from 69.53 to 73.67 at.%. Antimony is the second major component (13.63–24.87 at.%), and maximum contents of As, Sn, Te and Bi are 4.80, 5.25, 2.76 and 0.27 at.%, respectively. Representative compositions are given in Table 4.

Isomertieite and *mertieite I*, *both* [$Pd_{11}Sb_2As_2$]

Isomertieite (cubic) and mertieite I (hexagonal) are hard to distinguish optically (light yellowish white to brass or cream-yellow; anisotropy indistinct), have a Sb:As ratio near unity, and usually low contents of other elements besides Pd, As and Sb.

Isomertieite or mertieite I occur as large (up to 730 μm in diameter), single, homogeneous grains, and together with stibiopalladinite or mertieite II, as described above. In one case each, small (<5 μm) inclusions of gold and an attached grain of sperrylite (15 μm) were observed.

Chemically, the various grains of isomertieite or mertieite I have ΣPGE ranging from 71.74 to 74.53 at.%, and Pd contents are in the range 71.60 to 74.41 at.%. The grains are further characterized by restricted ranges of Sb and As contents (12.55 to 13.41 at.% Sb and 11.91 to 12.31 at.% As). The constant presence of low silver contents (up to 0.27 at.% Ag) is worthy of note. Representative compositions are given in Table 4.

Unnamed [$Pd_{11}Te_2As_2$]

A number of grains of this PGM were detected in the concentrates. The mineral occurs as large grains up to 150 μm across that contain oriented exsolution-induced bodies of keithconnite [$Pd_{3-x}Te$] intergrown with vasilite (Fig. 5d), and in polyphase grains (grain sizes between ~40 and 120 μm) together with Pt–Fe alloy, laurite, stillwaterite, cuprorhodsite, and other PGM (Figs. 7f, 4f and 5d). Chemically, the various grains of [$Pd_{11}Te_2As_2$] have ΣPGE ranging from 72.32 to 74.09 at.%, and Pd contents range from 72.30 to 74.01 at.%. Ranges of Te and As contents are 7.45 to 13.23 at.% Te and 10.01 to 13.45 at.% As. This mineral also contains up to (in at.%) 0.51 Se, 0.85 Sn, 4.57 Sb, 0.64 Pb and 0.39 Bi. The provisional formula [$Pd_{11}Te_2As_2$] was chosen following Törnroos *et al.* (1996), who described a chemically similar mineral from placers in Finnish Lapland. Representative compositions are given in Table 4.

Keithconnite [$Pd_{3-x}Te$]

Keithconnite was observed in the form of oriented exsolution-induced bodies in unnamed [$Pd_{11}Te_2As_2$] (Fig. 5d) and as a subordinate, small (10–30 μm) component in a number of polyphase grains (*e.g.*, Fig. 5e). The result of one analysis is given in Table 4.

Unnamed [Pd_3Fe]

Two small (~10 and 20 μm in diameter) grains of unnamed [Pd_3Fe] were found intergrown (i) in a complex grain consisting of Pt–Fe alloy, laurite, vasilite [$Pd_{16}S_7$], unnamed [$Pd_{11}Te_2As_2$], and unnamed RhFeNi sulfide (Fig. 7f), and (ii) in the form of a roundish inclusion, which is locally gold-bearing (3.77 at.% Au), in vasilite intergrown with unnamed [$Pd_{11}Te_2As_2$] that contains oriented exsolution-induced bodies of keithconnite [$Pd_{3-x}Te$] (Fig. 5d). Notably, Pd_3Fe is a stable phase in the system Pd–Fe–S, where it coexists with $Pd_{2.2}S$ (= "vasilite") at temperatures of 550 and 400°C (Makovicky & Karup-Møller 1993). Representative compositions are given in Table 5.

Zvyagintsevite [Pd_3Pb]

Zvyagintsevite is present (i) as a large (45 μm), homogeneous grain and a number of smaller inclusions at the periphery of an externally porous and internally compact grain of tulameenite with a small core of a remnant Pt–Fe grain, and (ii) as irregular, small grains in a coating of porous iron hydroxides on a grain of tulameenite. The textural siting of zvyagintsevite and its association with alteration phases of Pt–Fe alloy indicate that the mineral is secondary in origin and probably formed late in the sediments during weathering. One composition is given in Table 5.

Atokite [Pd_3Sn]

Grains of the atokite [Pd_3Sn] – rustenburgite [Pt_3Sn] solid-solution series are rare and were only observed as irregular or roundish inclusions, up to 20 μm in diameter, together with similar inclusions of moncheite [$PtTe_2$], sobolevskite [PdBi], and stibiopalladinite or mertieite I, in four grains of Pt–Fe alloy and tulameenite, and in one grain of gold (Fig. 7h). Chemically, all grains have (Pd > Pt) and are thus atokite. One representative composition is given in Table 5.

Unnamed [$(Pd,Rh)_3Te_2$]

This PGM was detected once only as an irregular rim 10–20 μm across and about 100 μm long along the periphery of a larger grain (200 μm in diameter) of Pt–Fe alloy that also carries inclusions of laurite and hollingworthite and has a partial rim of Rh–Fe–Ni sulfide. Kim (1990, pers. commun. 2003) confirmed the

phase Pd_3Te_2 in the synthetic system Pd–Te, which is stable up to 500°C. The composition (Table 4) shows that the formula of this mineral might also be written as [Pd_2RhTe_2].

Moncheite, michenerite, sobolevskite and kotulskite

Moncheite [$PtTe_2$], michenerite [PdBiTe], sobolevskite [PdBi] and kotulskite [PdTe] were only observed as small (<10 μm, rarely up to 50 μm) inclusions in stibiopalladinite and Pt–Fe alloy or intergrown with other PGM in complex grains.

Potarite

Individual detrital grains of potarite [PdHg] are rare and were only detected in the course of the SEM studies. However, a possible variant of potarite in the form of drop-like inclusions of a Cu-, Hg-, Ag- and Te-bearing palladium mineral in unnamed [Pd(Cu,Te)] also was found. Its composition is given in Table 5.

Unnamed [Pd(Cu,Te)]

Only one large grain of unnamed [Pd(Cu,Te)], 250 μm in diameter, was detected. The grain contains numerous drop- to emulsion-like inclusions of a Cu-, Hg-, Ag- and Te-bearing palladium mineral, possibly a variant of potarite [PdHg]. The unnamed [Pd(Cu,Te)] has a Pd:(Cu + Te) ratio near unity and might represent the Pd-dominant analogue of hongshiite [PtCu]. Compositions of [Pd(Cu,Te)] and the inclusions are given in Table 5.

Unnamed [Cu_2PdAu]

This phase was encountered only once in a complex grain mainly consisting of Pt–Fe alloy and attached laurite. The unnamed [Cu_2PdAu] is about 20 μm in diameter and is positioned close to the center of the complex grain. It is rimmed on one side by unnamed [Pd(Cu,Te)] and keithconnite, and on the other side by Rh–Fe–Ni sulfide. Udoh *et al.* (1986), cited by Prince *et al.* (1990), reported that an ordered phase with the composition ($AuCu_2Pd$) exists in the ternary system Au–Cu–Pd. According to Prince *et al.* (1990), the transformation temperature of ($AuCu_2Pd$) is about 550°C. The composition is given in Table 5.

Gold

Gold grains are internally homogeneous, though usually somewhat porous, and silver-rich (between 23.00 and 39.50 at.% Ag), and have an outer rim of variable thickness of silver-poor or pure gold (Fig. 5f). Other elements sought in gold (*e.g.*, Fe, Cu, Bi, Hg) are below their respective limits of detection. Two grains of Pd-rich gold (2.72 and 6.75 at.% Pd) were detected, and

TABLE 5. COMPOSITIONS OF VARIOUS PGM AND GOLD FOUND IN RIVERS DRAINING THE EASTERN BUSHVELD COMPLEX

Sample	Anal.	Mineral	Fe	Ni	Cu	Pd	Ag	Sn	Sb	Te	Pt	Au	Hg	Pb	Bi	Σ
AS6392	208	[Pd_3Fe]*	15.24		0.85	77.47					1.36	4.95	0.23			100.10
AS6444	152	[Pd_3Fe]*	16.13		1.82	83.69										101.64
AS6444	32	"Cu-potarite"			11.09	49.29	4.10			6.20			29.43	0.35		100.46
AS6444	34	Zvyagintsevite			0.13	60.40	0.23				1.39			39.90	0.11	102.16
AS6444	59	Atokite	1.34	0.17	1.02	37.43	0.11	17.97	0.20		38.70	1.37		3.19		101.50
AS6444	184	Atokite	1.23		0.81	48.24		22.20	0.47		27.27	1.55			0.24	102.02
AS6444	31	[Pd(Cu,Te)]*			32.80	60.10	0.11			7.49			1.58		0.13	102.20
AS6465	36	palladian Au	0.13		0.36	3.43					0.39	97.07				101.38
AS6465	10	[Cu_2PdAu]*	0.23		29.75	24.80				0.21	0.35	45.55		0.35		101.24
AS6392	208	[Pd_3Fe]*	1.04		0.05	2.78					0.03	0.10				4
AS6444	152	[Pd_3Fe]*	1.05		0.10	2.85										4
AS6444	32	"Cu-potarite"			0.40	1.06	0.09			0.11			0.34			2
AS6444	34	Zvyagintsevite			0.01	2.94	0.01				0.04			1.00		4
AS6444	59	Atokite	0.12	0.02	0.08	1.83	0.01	0.79	0.01		1.03	0.04		0.08		4
AS6444	184	Atokite	0.11		0.06	2.19		0.90	0.02		0.68	0.04			0.01	4
AS6444	31	[Pd(Cu,Te)]*			0.90	0.98				0.10			0.01			2
AS6465	36	palladian Au			0.01	0.06						0.92				1
AS6465	10	[Cu_2PdAu]*	0.02		1.99	0.99				0.01	0.01	0.98		0.01		4

S, Co, As, Se, Ru, Rh, Os, Ir and free fields: below detection limits. Compositions, derived from electron-microprobe analyses, are first expressed in weight %, then in atoms per formula unit, with the sum of atoms shown in the last column. * Unnamed species.

they carry some Pt (0.37 and 0.42 at.%) besides Ag (30.70 and 0.15 at.%), respectively. The most Pd-rich grain (composition $Au_{91}Pd_7$) is 20 μm in diameter and is attached to a complex grain consisting of Pt–Fe alloy, unnamed [$Pd_{11}Te_2As_2$] and sperrylite. One grain of gold contains numerous round to oval inclusions of atokite [Pd_3Sn], 1–5 μm in diameter (Fig. 7h), and another one has a larger inclusion of stibiopalladinite or mertieite II.

Base-metal sulfides, chromite and magnetite

Very rare inclusions of base-metal sulfides, mainly in Pt–Fe alloy, consist of pyrrhotite, chalcopyrite and cubanite. Although the concentrates contain numerous grains of chromite and magnetite, we found no intergrowths of the various PGM in them.

Discussion and Conclusions

The assemblage of detrital PGM comprises more than 40 different PGM and is therefore far more complex than anticipated with regard to (i) the wide variety and large number of different PGM identified, some of which are generally rare or even unnamed species, (ii) the complex and multiple intergrowths of the various PGM, (iii) the general dominance of Pt–Fe alloy grains, which are also present as one component in the majority of the polyphase grains, (iv) the presence of Ru-rich alloys, and (v) secondary alteration features.

Geological and geographical constraints indicate that the possible sources of the detrital PGM grains are the Merensky Reef, the UG–2 or other chromitite seams, or the platiniferous pipes of the Driekop or Mooihoek type, or yet unknown PGE occurrences. Cawthorn (2001) noted that the sedimentological history of the sand and gravel deposits on the farm Maandagshoek is not yet understood owing to Pliocene to Recent changes in the geomorphology of the area. According to Cawthorn (2001), significant rivers originally flowed southward, depositing considerable alluvium in the valleys. As a result of the recent uplift to the east, the Moopetsi River now contains a watershed running across the river valley on the farm Maandagshoek (Fig. 2). Accordingly, both a north- and a south-flowing Moopetsi River are present. In the area of the watershed, thick sediments of sand-supported gravels are present. These opposing streams on Maandagshoek are now reworking the Recent (or even older ?) poorly consolidated sediment accumulated prior to uplift. Therefore, the original, larger, south-flowing river could have eroded PGM from the Merensky Reef and the UG–2.

In his geochemical approach, Cawthorn (2001) hypothesized that the most probable source of the PGE in the placers is the Merensky Reef. This assumption was based on the Pt:Pd:Au proportions in the <250 μm sediment fraction, which showed similar element ratios as the Merensky Reef (Pt:Pd:Au ≈ 6:3:1). However, the relationship is not that straightforward owing to the fact that secondary alteration of PGM in the weathering environment preferentially removes Pd relative to Pt, as already shown by Wagner (1929) for the Merensky Reef. Cousins & Kinloch (1976) gave Pt/Pd values of 2.7 for sulfide ore and 5.1 for oxidized ore of the Merensky Reef. For the UG–2 from the Union section, Hey (1999) provided Pt/Pd values of 2.2 for primary and up to 3.2 for oxidized ore. Similar relationships between pristine and oxidized PGE mineralization, namely average Pt/Pd values of 1.28 and 2.43, respectively, were reported from the Main Sulfide Zone of the Great Dyke in Zimbabwe (Oberthür *et al.* 1998, 2003, Oberthür 2002). In conclusion, the geochemical data obtained from the sediments do not contain unequivocal fingerprints of the sources.

The ores of the Bushveld Complex constitute the world's largest resource in PGE, and a very large mineralogical database has been accumulated by the mining companies. However, no concise, state-of-the-art account of the mineralogy of the primary PGM assemblages is available. Therefore, reference had to be made to older, somewhat partly outdated or imprecise literature, especially regarding PGM nomenclature. Generally, the PGM assemblages recorded from the Merensky Reef and the UG–2 have high mineralogical variability and differ between various localities and facies of the reefs. In approximate order of abundance, cooperite and braggite, Pt–Fe alloy, sperrylite and laurite are common constituents in both types of ore (Vermaak & Hendricks 1976, Cousins & Kinloch 1976, Kingston & El-Dosuky 1982, Kinloch 1982, McLaren & De Villiers 1982, Mostert *et al.* 1982, Hey 1999, Cawthorn *et al.* 2002). Additional PGM are various bismuthotellurides (*e.g.,* moncheite, merenskyite, michenerite), sulfarsenides (*e.g.*, hollingworthite, platarsite), and many rare PGM, mainly compounds of Pt or Pd with As, Sb and Te. Notably, an undefined Pt–Rh–Cu sulfide is also present in both the Merensky Reef and the UG–2 (Kinloch 1982, Penberthy & Merkle 1999, Hey 1999) and may achieve elevated proportions locally (*e.g.*, 11% of the PGM by area in the UG–2 at Union section; Hey 1999). All authors cited above agree that the grain sizes of the PGM are much larger in the Merensky Reef (~10–200 μm, even up to 1 mm) compared to those of the UG–2 (<10–30 μm).

The PGM assemblages of the platiniferous pipes stand in distinct contrast to those of the Merensky Reef and the UG–2. Wagner & Mellor (1925) described Pt–Fe nuggets in the form of cubic crystals and irregular particles up to 5 mm in size from the eluvial gravels surrounding the Mooihoek and Onverwacht pipes. Stumpfl (1961, 1974) and Tarkian & Stumpfl (1975) reported Pt–Fe alloy (50%), geversite [$PtSb_2$] and sperrylite (together 30%), hollingworthite and irarsite (15%), and other PGM (5%) including stibiopalladinite, laurite, Os–Ir alloy, and native gold from Driekop. PGE sulfides are rare, and PGE bismuthotellurides are absent. Grain sizes of Pt–Fe alloy grains reach up to 1 mm,

and other PGM are up to several 100 μm across (Tarkian & Stumpfl 1975). Cabri *et al.* (1977a, b, c) described Pt–Fe alloy, various Pt–Fe–Cu–Ni alloys, platarsite [PtAsS], genkinite [$(Pt,Pd)_4Sb_3$], sperrylite, stibiopalladinite, ruthenarsenite [RuAs], and mertieite II from the Onverwacht deposit. The scarcity to absence of PGE sulfides and bismuthotellurides is characteristic. Rudashevsky *et al.* (1992) reported nearly 20 different PGM, *e.g.*, Pt–Fe alloy, sperrylite, hollingworthite, platarsite, laurite and some rarer species, with grain sizes up to about 100 μm from the Mooihoek and Onverwacht pipes. These authors identified several PGM assemblages, which they interpreted to be products of different ore-forming stages, from magmatic to subsolidus to auto-metamorphic, with the participation of a metal-bearing fluid. Ru-rich alloy was so far only reported by Merkle (1998) from the UG–1 chromitite, and Zaccarini *et al.* (2002) found laurite, Pt–Fe alloy, Ru alloy ($Ru_{77–80}$), sperrylite, hollingworthite, Rh–Pd–Ru arsenides, and an undefined Pd–Sb compound with grain sizes mostly <10 μm and exceptionally up to 200 μm in chromitite xenoliths from the pipes of Onverwacht and Tweefontein (*ca*. 30 km south–southwest of Onverwacht). Zaccarini *et al.* (2002) stated that the scarcity of PGM sulfides and the common occurrence of As-bearing species and PGE alloys are ubiquitous features of the platiniferous dunites, the chromitite xenoliths, and the metasomatized fragments of chromitite found in the pipes, and concluded that these features indicate crystallization at low $f(S_2)$ and relatively high As:S ratio, *i.e.*, in a sulfur-poor environment.

The assemblage of detrital PGM consists of individual grains that display morphologies indicative of either subordinate or strong physical abrasion and wear, and also either negligible or severe chemical alteration. These different states of preservation probably point to long-lived, continuous erosion and accumulation of the PGM by sedimentological processes. The grain sizes of the detrital PGM are all >40 μm, mainly in the range 100–200 μm, and even up to 1.6 mm in diameter, in contrast to the primary PGM of the Merensky Reef and the UG–2, which are mostly <50 μm. These differences in grain sizes between primary and placer PGM are not regarded a major obstacle; it is assumed that sedimentological sorting led to the concentration of the rare larger grains.

The suite of detrital PGM identified, namely major Pt–Fe alloy, sperrylite and laurite, as well as a number of rarer PGM arsenides and sulfarsenides, are common to the Merensky Reef, the UG–2, and the platiniferous pipes. Cooperite, braggite and PGE tellurides are main constituents, and Rh sulfides are rarer constituents of the Merensky Reef and the UG–2, but are unknown from the platiniferous pipes. Ru-rich alloy, quite prominent as detrital PGM, has so far only been reported as small and rare constituents from the Onverwacht and Tweefontein pipes. In analogy to detrital grains of multicomponent alloys of Os–Ir–Ru–Rh–Pt found in the Somabula gravels of Zimbabwe (Oberthür *et al.* 2002a), we suggest that the Bushveld multicomponent PGE alloys described above formed from complex PGE-dominant solid solutions at low sulfur fugacities.

In conclusion, the geomorphological, geological, sedimentological, geochemical and mineralogical constraints deliver equivocal direct links to the single or multiple sources of the detrital PGM. The PGM assemblage may therefore represent a mixture in variable proportions originating from the Merensky Reef, the UG–2, the platiniferous pipes, or still undetected occurrences of PGE and PGM. In spite of a number of unsolved questions, the presence as such of detrital PGM in general and of a large number of both rare and hitherto unreported PGM in the sediments has significant implications. Our work has shown that the combination of "old-fashioned" field techniques and modern analytical methods has the capability to outline placer accumulations of PGE, which may have economic potential, and are valuable tools to obtain indications toward primary PGE sources in projects of regional mineral exploration. Furthermore, in case the PGM unreported so far originate from currently exploited horizons like the Merensky Reef or the UG–2, then they have been overlooked in the past. Their recognition in the primary ores may improve the metallurgical treatment of the ores and bear consequences regarding the genetic understanding and interpretation of the mineralization. Further fingerprints of the sources of the detrital PGM may be obtained from future mineralogical studies of the exploited PGE-bearing ores of the eastern Bushveld, and the unravelling of the redistribution processes involving the primary PGM, during weathering, sedimentary transport and subsequent to deposition.

The area of the farm Maandagshoek and environs has proven to be a world-unique "hot spot" with regard to PGE mineralization and mineralogy. The most valuable and interesting types of PGE mineralization of the Bushveld Complex are present, namely the economic horizons of the Merensky Reef and the UG–2, the platiniferous pipes, and PGM placers. The larger area embraces the type localities of a number of PGM, *e.g.*, atokite [Pd_3Sn] (Atok mine), geversite [$PtSb_2$] and stumpflite [PtSb] (Driekop pipe), tetraferroplatinum [PtFe] (Mooihoek pipe), genkinite [$(Pt,Pd)_4Sb_3$] and platarsite [PtAsS] (Onverwacht pipe), not to forget mooihoekite [$Cu_5Fe_9S_{16}$] and merenskyite [$PtTe_2$]! Amazingly, nearly 80 years after the initial discovery of economic PGE mineralization in the Bushveld Complex in 1924, these classic occurrences still bear some surprises.

Acknowledgements

We are most grateful to Grant Cawthorn, who guided us in the field, significantly improved the local logistics of our field work, gave continuous advice and provided fruitful discussions. Many thanks go to AngloPlatinum

(R. Hieber, C. Lee) for allowing access to their property. Ms. E. Brinkmann (BGR) ably drafted Figure 2. The paper experienced considerable improvement through critical reviews and valuable suggestions by Louis Cabri, Chusi Li and Roland Merkle as well as the editorial comments of Robert F. Martin. The work would not have been possible without the extraordinary skills of Gilles Laflamme of CANMET, who provided excellent polished sections of the single hand-picked PGM grains. Special thanks, Gilles!

REFERENCES

ATANASOV, A.V. (1990): Vasilite, $(Pd,Cu)_{16}(S,Te)_7$, a new mineral species from Novoseltsi, Bulgaria. *Can. Mineral.* **28**, 687-689.

BEGIZOV, V.C., MESHCHANKINA, V.I. & DUBAKINA, L.S. (1974): Palladoarsenide, Pd_2As, a new natural palladium arsenide from the copper–nickel ores of the Oktabyr deposit. *Int. Geol. Rev.* **16**, 1294-1297.

CABRI, L.J. (2002): The platinum-group minerals. *In* The Geology, Geochemistry, Mineralogy and Mineral Beneficiation of Platinum-Group Elements (L.J. Cabri, ed.). *Can. Inst. Mining, Metall. Petroleum, Spec. Vol.* **54**, 13-129.

_____, CRIDDLE, A.J., LAFLAMME, J.H.G., BEARNE, G.S. & HARRIS, D.C. (1981): Mineralogical study of complex Pt–Fe nuggets from Ethiopia. *Bull. Minéral.* **104**, 508-525.

_____, LAFLAMME, J.H.G. & STEWART, J.M. (1977b): Platinum-group minerals from Onverwacht. II. Platarsite, a new sulfarsenide of platinum. *Can. Mineral.* **15**, 385-388.

_____, ROSENZWEIG, A. & PINCH, W.W. (1977a): Platinum-group minerals from Onverwacht. I. Pt–Fe–Cu–Ni alloys. *Can. Mineral.* **15**, 380-384.

_____, STEWART, J.M., LAFLAMME, J.H.G. & SZYMAŃSKI, J.T. (1977c): Platinum-group minerals from Onverwacht. III. Genkinite, $(Pt,Pd)_4Sb_3$, a new mineral. *Can. Mineral.* **15**, 389-392.

CAWTHORN, R.G. (1999): The discovery of the platiniferous Merensky Reef in 1924. *S. Afr. J. Geol.* **102**, 178-183.

_____ (2001): A stream sediment geological re-investigation of the discovery of the platiniferous Merensky Reef, Bushveld Complex. *J. Geochem. Explor.* **72**, 59-69.

_____, LEE, C.A., SCHOUWSTRA, R.P. & MELLOWSHIP, P. (2002): Relationship between PGE and PGM in the Bushveld Complex. *Can. Mineral.* **40**, 311-328.

COUSINS, C.A. & KINLOCH, E.D. (1976): Some observations on textures and inclusions in alluvial platinoids. *Econ. Geol.* **71**, 1377-1398.

DALTRY, V.D.C. & WILSON, A.H. (1997): Review of platinum-group mineralogy: compositions and elemental associations of the PG-minerals and unidentified PGE-phases. *Mineral. Petrol.* **60**, 185- 229.

GAIN, S.B. (1985): The geologic setting of the platiniferous UG2 chromitite layer on the farm Maandagshoek, eastern Bushveld Complex. *Econ. Geol.* **80**, 925-943.

GAST, L. & WITTICH, C. (2001): Detritische Platingruppenminerale im Eastern Bushveld, Republik Südafrika – eine Reconnaissance-Beprobung. *Archive of the Bundesanstalt für Geowissenschaften und Rohstoffe* (*BGR*), *Hannover, Archive-No.* **0120650**.

HAGEN, D., WEISER, TH. & THAN HTAY (1990): Platinum-group minerals in Quaternary gold placers in the upper Chindwin area of northern Burma. *Mineral. Petrol.* **42**, 265-286.

HEY, P.V. (1999): The effects of weathering on the UG2 chromitite reef of the Bushveld Complex, with special reference to the platinum-group minerals. *S. Afr. J. Geol.* **102**, 251-260.

KARUP-MØLLER, S. & MAKOVICKY, E. (1999): The phase system Cu–Pd–S at 900°, 725°, 550° and 400°. *Neues Jahrb. Mineral., Monatsh.*, 551-567.

KIM, WON-SA (1990): Phase relations in the Pd–Te system. *J. Less-Common Metals* **162**, 61-74.

KINGSTON, G.A. & EL-DOSUKY, B.T. (1982): A contribution on the platinum-group mineralogy of the Merensky Reef at the Rustenburg Platinum mine. *Econ. Geol.* **77**, 1367-1384.

KINLOCH, E.D. (1982): Regional trends in the platinum-group mineralogy of the Critical Zone of the Bushveld Complex, South Africa. *Econ. Geol.* **77**, 1328-1347.

MAKOVICKY, E. (2002): Ternary and quaternary phase systems with PGE. *In* The Geology, Geochemistry, Mineralogy and Mineral Beneficiation of Platinum-Group Elements (L.J. Cabri, ed.). *Can. Inst. Mining, Metall. Petroleum, Spec. Vol.* **54**, 131-175.

_____ & KARUP-MØLLER, S. (1993): The system Pd–Fe–S at 900°, 725°, 550° and 400°. *Econ. Geol.* **88**, 1269-1278.

MCLAREN, C.H. & DE VILLIERS, J.P.R. (1982): The platinum-group chemistry and mineralogy of the UG–2 chromitite layer of the Bushveld Complex. *Econ. Geol.* **77**, 1348-1366.

MELCHER, F. (2000): Base metal – platinum-group element sulfides from the Urals and the Eastern Alps: characterization and significance for mineral systematics. *Mineral. Petrol.* **68**, 177-211.

MERENSKY, H. (1924): The various platinum occurences on the farm Maandagshoek No. 148. Unpublished memorandum to Lydenburg Platinum Syndicate. Archives of the Merensky Trust, Duivelskloof, South Africa.

_____ (1926): Die neuentdeckten Platinfelder im mittleren Transvaal und ihre wirtschaftliche Bedeutung. *Z. Deutsch. Geol. Gesellsch.* **78**, 296-314.

MERKLE, R.K.W. (1998): Proportions of magmatic platinum-group minerals and evolution of mineralizing processes,

UG–1 chromitite layer, Bushveld Complex. *In* International Platinum (N.P. Laverov & V.V. Distler, eds.). Theophrastus Publications, St. Petersburg, Russia (43-53).

MOSTERT, A.B., HOFMEYR, P.K. & POTGIETER, G.A. (1982): The platinum-group mineralogy of the Merensky Reef at the Impala Platinum mines, Bophuthatswana. *Econ. Geol.* **77**, 1385-1394.

OBERTHÜR, T. (2002): Platinum-group element mineralization of the Great Dyke, Zimbabwe. *In* The Geology, Geochemistry, Mineralogy and Mineral Beneficiation of Platinum-Group Elements (L.J. Cabri, ed.). *Can. Inst. Mining, Metall. Petroleum, Spec. Vol.* **54**, 483-506.

_____, MELCHER, F., GAST, L., WÖHRL, C. & LODZIAK, J. (2002b): Detrital platinum-group minerals (PGM) in rivers of the Bushveld Complex, South Africa – a reconnaissance study. *In* Ninth Int. Platinum Symp., Ext. Abstr. (A. Boudreau, ed.), 329-332.

_____, WEISER, TH.W., GAST, L. & KOJONEN, K. (2003): Geochemistry and mineralogy of the platinum-group elements at Hartley platinum mine, Zimbabwe. 2. Supergene redistribution in the oxidized Main Sulfide Zone of the Great Dyke, and alluvial platinum-group minerals. *Mineral. Deposita* **38**, 344-355.

_____, _____, _____, LODZIAK, J., KLOSA, D. & WITTICH, C. (1998): Detrital platinum group minerals in rivers along the Great Dyke, and in the Somabula gravels, Zimbabwe. *In* Eighth Int. Platinum Symp. *S. Afr. Inst. Mining Metall., Symp. Ser.* **S 18**, 289-292.

_____, _____, _____, SCHOENBERG, R. & DAVIS, D.W. (2002a): Platinum-group minerals and other detrital components in the Karoo-age Somabula gravels, Gweru, Zimbabwe. *Can. Mineral.* **40**, 435-456.

PARTRIDGE, T.C. (1998): Of diamonds, dinosaurs and diastrophism: 150 million years of landscape evolution in southern Africa. *S. Afr. J. Geol.* **101**, 165-184.

PENBERTHY, C.J. & MERKLE, R.K.W. (1999): Lateral variations in the platinum-group element content and mineralogy of the UG–2 chromitite layer, Bushveld Complex. *S. Afr. J. Geol.* **102**, 240- 250.

PRINCE, A., RAYNOR, G.V. & EVANS, D.S. (1990): *Phase Diagrams of Ternary Gold Alloys*. Institute of Metals, London, U.K. (233-241).

RUDASHEVSKY, N.S., AVDONTSEV, S.N. & DNEPROVSKAYA, M.B. (1992): Evolution of PGE mineralization in hortonolitic dunites of the Mooihoek and Onverwacht pipes, Bushveld Complex. *Mineral. Petrol.* **47**, 37-54.

SCHNEIDERHÖHN, H. & MORITZ, H. (1939): Die Oxydationszone im platinführenden Sulfidpyroxenit (Merensky-Reef) des Bushvelds in Transvaal. *Zentralbl. Mineral. Geol. Paläontol., Abteilung A*, 1-12.

STUMPFL, E.F. (1961): Some new platinoid-rich minerals, identified with the electron microanalyser. *Mineral. Mag.* **32**, 833-847.

_____ (1974): The genesis of platinum deposits: further thoughts. *Minerals Science Engineering* **6**, 120-141.

TARKIAN, M., KRSTIC, S., KLASKA, K.-H. & LIESSMANN, W. (1997):. Rhodarsenide, $(Rh,Pd)_2As$, a new mineral. *Eur. J. Mineral.* **9**, 1321-1325.

_____ & STUMPFL, E.F. (1975): Platinum mineralogy of the Driekop mine, South Africa. *Mineral. Deposita* **10**, 71-85.

TÖRNROOS, R., JOHANSON, B. & KOJONEN, K. (1996): Alluvial nuggets of platinum-group minerals and alloys from Finnish Lapland. *Geol. Surv. Finland, Spec. Pap.* **26**, 63-64.

UDOH, K., YASUDA, K. & YAMAUCHI, H. (1986): Cu–Au–Pd phase diagram. *Metall. Soc. AIME, TMS Tech. Pap.* **A86-37**, 1-10.

VERMAAK, C.F. & HENDRICKS, L.P. (1976): A review of the mineralogy of the Merensky Reef, with specific reference to new data on the precious metal mineralogy. *Econ. Geol.* **71**, 1244-1269.

VERRYN, S.M.C. & MERKLE, R.K.W. (1994): Compositional variation of cooperite, braggite, and vysotskite from the Bushveld Complex. *Mineral. Mag.* **58**, 223-234.

_____ & _____ (2002): The system PtS–PdS–NiS between 1200° and 700°C. *Can. Mineral.* **40**, 571-584.

WAGNER, P. (1929): *The Platinum Deposits and Mines of South Africa*. Oliver & Boyd, Edinburgh, U.K.

_____ & MELLOR, E.T. (1925): On platinum-bearing hortonolite–dunite of the Lydenburg district. *Trans. Geol. Soc. S. Afr.* **28**, 1-17.

WEISER, TH.W. (2002): Platinum-group minerals (PGM) in placer deposits. *In* The Geology, Geochemistry, Mineralogy and Mineral Beneficiation of Platinum-Group Elements (L.J. Cabri, ed.). *Can. Inst. Mining, Metall. Petroleum, Spec. Vol.* **54**, 721-756.

ZACCARINI, F., GARUTI, G. & CAWTHORN, R.G. (2002): Platinum-group minerals in chromite xenoliths from the Onverwacht and Tweefontein ultramafic pipes, eastern Bushveld Complex, South Africa. *Can. Mineral.* **40**, 481-497.

Received March 23, 2003, revised manuscript accepted October 17, 2003.